

Hydrophobic carbon dots: An overview of the synthesis, purification, cytotoxicity, and potential applications in food safety and analytical chemistry

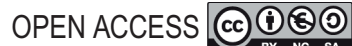
Rahim Molaei^{1*}, Roghayieh Razavi², Abdullah Khalid Omer², Anita Lotfi Javid², Parya Ezati³, Negar Nikfarjam⁴, Loong-Tak Lim³, Mehran Moradi^{2*}

¹Materials Synthesis Laboratory, Carbon Tech Industrial Group, Carbon Tech, Urmia, Iran; ²Department of Food Hygiene and Quality Control, Faculty of Veterinary Medicine, Urmia University, Urmia, Iran; ³Department of Food Science, University of Guelph, Canada; ⁴Faculty of Veterinary Medicine, University of Tehran, Tehran, Iran

*Corresponding Authors: Rahim Molaei, Materials Synthesis Laboratory, Carbon Tech Industrial Group, Carbon Tech, Urmia, Iran. Email: rahimmolaie@yahoo.com; and Mehran Moradi, Department of Food Hygiene and Quality Control, Faculty of Veterinary Medicine, Urmia University, Urmia, Iran. Email: m.moradi@urmia.ac.ir

Academic Editor: Sedat Sayar, PhD., Department of Food Engineering, Mersin University, Mersin, Turkey

Received: 20 October 2024; Accepted: 6 February 2025; Published: 1 April 2025 © 2025 Codon Publications



REVIEW PAPER

Abstract

Hydrophobic carbon dots (HCDs) represent a burgeoning class of nanomaterials distinguished by their unique physicochemical, antimicrobial, and optical properties. These attributes have propelled HCDs to the forefront of research, particularly in the fields such as composite film production, biological imaging, and antibacterial coatings, with broad implications for industries, such as food safety, medicine, catalysis, and sensor technology. This comprehensive review delves into the diverse synthesis methodologies of HCDs, such as chemical oxidation, hydrothermal/solvothermal techniques, pyrolysis, and microwave irradiation. The comparative benefits and challenges of these methods were analyzed critically. This manuscript presents an in-depth exploration of purification methods, hydrophobicity indices, and cytotoxicity by a thorough examination of current literature. In addition, it highlights the innovative applications of HCDs, from advanced chemosensors, the development of stationary phases for chromatography to bioimaging and diagnostics, and the construction of optoelectric devices for food applications.

Keywords: hydrophobic carbon dots; synthesis methods; purification techniques; cytotoxicity; sensors; bioimaging

Introduction

Carbon dots (CDs) are sustainable and highly functional nanoparticles. Their sub-10-nanometer size, high stability, low cytotoxicity, tunable photoluminescence (PL) properties, high quantum yields, availability of diverse precursors, and simplicity in synthesis techniques make them favorable for many applications over other carbon-based nanomaterials (Chu *et al.*, 2019; Yin *et al.*, 2019). Moreover, their carbonaceous core with

sp²/sp³ hybridization can be functionalized with amine, epoxy, ether, carbonyl, carboxyl, and hydroxyl or doped with heteroatoms (e.g., N, P, S, and B), thereby providing many opportunities for the fabrication of novel nanomaterials (Garg et al., 2022; Raveendran and Kizhakayil, 2021). These diverse surface functional groups make them hydrophilic, hydrophobic, or amphiphilic, which significantly influences their solubility and dispersibility in various media and provides diversity to the scope of their applications (Shang et al., 2018). However, a notable

challenge with hydrophilic CDs is fluorescence quenching due to aggregation and strong intermolecular ' π – π ' stacking among adjacent surface groups during the fabrication of solid-state fluorescent CDs for optoelectronic devices and fluorometric sensors (Bandi *et al.*, 2020; Pagidi *et al.*, 2022).

To address this issue, hydrophobic surface functional groups (such as aliphatic carbons/ligands) can be employed, allowing CDs to be effectively dispersed in organic solvents and enhancing their compatibility with organic electronic materials. Hydrophobic carbon dots (HCDs) can be dispersed in a wide range of organic solvents (De et al., 2021). Extensive research has focused on developing and understanding HCDs for various technological applications. The methodology of synthesis for HCDs has been a focal point of investigation, with various techniques being developed to tailor the properties of HCDs to meet specific application requirements. Cytotoxicity studies have shown that HCDs generally exhibit low toxicity toward mammalian cells, making them suitable for biomedical applications. HCDs have the potential to be incorporated into polymer matrix structures for use in the fields of food, drug delivery, and medicine (Fu et al., 2022b; Jiang et al., 2021). HCDs have been incorporated into polydimethylsiloxane (PDMS) (Kováčová et al., 2020; Yang et al., 2022), polycaprolactone (PCL) (Budimir et al., 2021), polyurethane (PU) (Zhang et al., 2024), poly(methyl methacrylate) and polydimethylsiloxane (Yin et al., 2019), polyester (Chu et al., 2022), and amphiphilic polymers (1,2-distearoylsn-glycero-3-phosphoethanolamine-N-methoxy ethylene glycol) (Yang et al., 2016). HCDs have shown utility as chemosensors for the detection of various analytes, as the surface functional groups of HCDs can interact with specific molecules, leading to changes in their fluorescence properties. Chemosensors based on HCDs are used for environmental monitoring, food safety, and medical diagnostics, providing rapid and accurate detection of harmful substances, including heavy metals, toxins, and biomolecules. In addition, studies have revealed the efficacy of HCDs in inhibiting microbial growth and in preventing biofouling on surfaces. These properties make HCDs highly effective as antimicrobial agents for various applications, including medical devices, water purification, and food packaging.

This paper is a comprehensive overview of the synthesis methods, antimicrobial properties, cytotoxicity considerations, and potential applications of HCDs in food safety and analytical chemistry. This review offers valuable insights to researchers and practitioners seeking to harness the unique properties of HCDs for novel technological applications. The development of environment-friendly synthesis methods, optimization of surface functionalization, and thorough evaluation

of biocompatibility and safety profiles are crucial steps toward realizing the full potential of HCDs.

Synthesis of HCDs

Carbon dots are produced by top-down and bottom-up approaches (Moradi et al., 2023). This classification relies on the size relationship between CDs and type of precursor (Shi et al., 2019). Laser ablation is a top-down approach for preparing CDs that is rapid and straightforward to deploy, although the process is energy-intensive, which restricts its widespread use. In addition, CDs produced using this method have low quantum yield (Li et al., 2021a). However, synthesis through electrochemical oxidation can result in high purity and yield, although the processing steps are complex (Das et al., 2018). Other methods, such as the sonochemical approach, are novel, facile, and simple, involving mild experimental conditions for the production of CDs with controlled physicochemical properties, although the lack of control over the particle size hampers its applicability in large-scale and widespread production (Dutta and Karak, 2022; Kumar et al., 2020). HCDs are synthesized using hydrophobic precursors, partial carbonization of organic materials, and secondary surface modification of water-soluble CDs with amphiphilic molecules (Yao et al., 2019). Information regarding the precursors, solvents, and methods of synthesis of HCDs is presented in Table 1.

Chemical oxidation approach

It is a straightforward approach for the large-scale preparation of CDs; however, one drawback of this method is the lack of homogeneity in the particles produced (Bartolomei et al., 2021). This method was used by Lin et al. (2022) for the synthesis of HCDs from triolein. They mixed triolein and concentrated sulfuric acid in ethyl acetate, followed by vigorous stirring for 2 h under ambient conditions. The hydrophobic product was separated and precipitated after liquid-liquid extraction, followed by the neutralization of organic phase with NaHCO3 solution. Zheng et al. (2015) reported the synthesis of HCDs using cetylpyridinium chloride monohydrate (CPC) and sodium hydroxide. In their green one-step method, CPC was mixed with NaOH (0.0 to 360 mM) for various reaction periods (28 to 180 h) at room temperature. They showed that longer reaction period and higher initial NaOH concentrations led to the production of higher quantities of HCDs (Figure 1A). Feng et al. (2020) used terephthalaldehyde, dimethyl formamide, pyrrole, and trifluoroacetic acid as raw materials (Figure 1B). Redemitting HCDs were obtained by stirring the mixture at room temperature for 120 h. The synthesized HCDs

Precursors	Synthesis method	Extraction/purification	Method of characterization	Application	Reference
Deep eutectic solvent and molasses	Hydrothermal (300°C for 75 min)	Water-wash method, centrifugation; solvent extraction	HRTEM < 20 nm; UV-vis spectroscopy, PLPL; Zeta potential; FTIR; XRD	ı	Çalhan <i>et al.</i> , 2018
Pluronic F-68 and o-phosphoric acid	Microwave assisted (450 W for 4 min)	Solvent extraction	HRTEM and TEM; 5–20 nm; UV-vis spectroscopy, PL; FTIR; XRD; AFM; SAED	ı	Mitra <i>et al.</i> , 2012
Hexane, dextran sulfate sodium salt from Leuconostoc spp, (polyoxyethylene (4) lauryl ether, water	Solvothermal (180°C for 3 h)	ı	TEM; 5.0 nm; PL Raman	ı	Prikhozhdenko et al., 2018
Citric acid, ethanol, $C_{1g}H_{37}$ NH_3^+	Pyrolysis 300°C for 2 h	Solvent extraction	TEM; 3–15 nm; UV-vis spectroscopy; PL; FTIR; XRD; TGA	1	Bourlinos <i>et al.</i> , 2008
Lauryl gallate	Pyrolysis 270°C for 2 h	Solvent extraction; filtration	TEM; 3–15 nm; UV-vis spectroscopy; PL	1	Bourlinos et al., 2013
Pluronic F-68 and o-phosphoric acid	Solvothermal (250°C for 2 h)	Solvent extraction	HRTEM and TEM; 5 nm; UV-vis spectroscopy PL; XPS; FTIR; AFM; SAED	Antibacterial and Antibiofouling	Stanković <i>et al.</i> , 2018
Pluronic F-68 and o-phosphoric acid	Solvothermal (250°C for 2 h)	Solvent extraction	HRTEM and TEM; 5 nm; UV-vis spectroscopy; PL; XPS; FTIR; AFM	Antibacterial photodynamic activity (in polydimethylsiloxane nanocomposite)	Marković <i>et al.</i> , 2019
Pluronic F-68 and o-phosphoric acid	Solvothermal (250°C for 2 h)	Solvent extraction		Antibacterial surface coating (in composite with polyetherurethane and polyester urethane)	Kováčová <i>et al.</i> , 2020
Riboflavin, ethylenediamine, acetone	Hydrothermal (180°C for 12 h)	Centrifugation; filtration	HRTEM and TEM; 20 nm; UV-vis spectroscopy; PL XPS; FTIR; EDS	Antimicrobial film	Marković <i>et al.</i> , 2022
Ionic liquids EMIMBF4, BMIMBF4, HMIMBF4, OMIMBF4, DMIMBF4, sulfuric acid, ethanol	Hydrothermal (200°C for 48 h)	Centrifugation; dialysis	HRTEM; 5.8 nm; UV-vis spectroscopy; PL; XPS; FTIR; XRD	Anticancer drug curcumin delivery system	Shu <i>et al.</i> , 2017
1-Alkyl-3-methylimidazolium dicyanamide	Microwave-assisted (490 W for 5 min)	Centrifugation; dialysis	TEM; ~9–10 nm; UV-vis spectroscopy; PL; FTIR; Zeta potential; DLS	Cell imaging	Guo <i>et al.</i> , 2022
Sucrose, dodecylamine, ethanol	Solvothermal (210°C for 10 min)	Solvent extraction, centrifugation	HRTEM and TEM; ~3–9 nm; UV-vis spectroscopy; photoluminescence; XPS; FTIR	Lipid raft marker	Chatterjee <i>et al.</i> , 2022
Terephthalaldehyde, DMF, pyrrole, trifluoroacetic acid	Chemical carbonization for 120 h	Silica gel column chromatography	HRTEM; 5.70 nm; UV-vis spectroscopy; PL; XPS; FTIR	Bio-imaging	Feng <i>et al.</i> , 2020
					(continues)

Table 1. Continued.					
Precursors	Synthesis method	Extraction/purification	Method of characterization	Application	Reference
Paraplast, toluene, and dodecanethiol	Hot injection (nitrogen flushed)	Filtration (0.2 µm)	HRTEM; 5–30 nm; UV-vis spectroscopy XRD; FTIR; Raman	Biological imaging of cancer stem cells	Talib <i>et al.</i> , 2015
1-Butyl-3-methylimidazolium hexafluorophosphate, phosphoric acid, and ethanol	Hydrothermal (200°C, 96 h)	Centrifugation; dialysis	HRTEM; 6.1 nm; UV-vis spectroscopy; PL; XPS; XRD; FTIR	Bio-imaging/bio-labeling	Mao e <i>t al.</i> , 2015
Variety of carbohydrates, octadecylamine, and octadecene	Solvothermal (70–300°C for 10–30 min)	Solvent extraction column chromatography	TEM; 1–10 nm; UV-vis spectroscopy; PL; XPS; XRD; FTIR; DLS	Cell imaging probes	Bhunia <i>et al.</i> , 2013
1-Alkyl-3-methylimidazolium dicyanamide, ethanol	Microwave-assisted (490 W for 5 min)	Centrifugation; dialysis	TEM; <12 nm; UV-vis spectroscopy; PL; FTIR; XPS; WCA	Bio-imaging	Guo <i>et al.</i> , 2021
1-Ethly-3-methylimidazolium, phosphoric acid, and ethanol	Hydrothermal (230°C, 24 h)	Centrifugation; dialysis	HRTEM; 8.52+1.61 nm; UV-vis spectroscopy; PL; XPS; FTIR; XRD	In vitro and in vivo imaging	Mao e <i>t al.</i> , 2016
L-ascorbic acid and oleylamine	Solvothermal (280°C for 4 h)	Solvent extraction	TEM; 3–8 nm UV-vis spectroscopy; PL; XPS; FTIR; XRD; DLS; Raman	Cell Imaging probe	Ali et al., 2016
Cetylpyridinium chloride monohydrate and sodium hydroxide	Chemical carbonization	Solvent extraction Dialysis	TEM; 6.2 nm; UV-vis spectroscopy; PL; XPS; FTIR	Bio-imaging	Zheng <i>et al.</i> , 2015
1,3,6-Trinitropyrene, ethanol, DMF	Solvothermal (230°C for 12 h)	Filtration (0.22 µm)	TEM; <4 nm; UV-vis spectroscopy; PL; XPS; FTIR; XRD; Raman	In vivo and in vitro imaging	Zhan et al., 2018
2,6-Dibromo naphthalene dianhydride and ethylene glycol	Solvothermal (220°C for 3.5 h)	Water-wash method; centrifugation; dialysis	TEM; 6.1 nm; UV-vis spectroscopy; PL; XPS; FTIR	Imaging of lipid droplets inside the living cells	Paul <i>et al.</i> , 2022
Urea, citric acid in anhydrous DMF, octylamine, N,N'-dicyclohexylcarbodiimid, and N-hydroxysuccinimide	Functionalized of CDs	Centrifugation; dialysis	HRTEM; 4.4 ± 0.8 nm; FTIR; 1H-NMR; AFM; Zeta potential	Bio-imaging	Mauro et al., 2021
Pheophytin powders, N,N-dimethylformamide	Microwave-assisted (150°C for 30 min)	Filtration	TEM; 5.5 nm; UV-vis spectroscopy; PL; Zeta potential; XPS	Bioimaging and photodynamic therapy	Wen <i>et al.</i> , 2019
Clitoria ternatea leaves, dichloromethane	Hydrothermal (160°C for 24 h)	Filtration (0.22 µm)	TEM; 5–10 nm; UV-vis spectroscopy; PL; XPS; FTIR	Bioimaging and synergistic phototherapy in breast cancer	Shinde <i>et al.</i> , 2023
Cu(acac) ₂ , MoO ₂ Cl ₂ , and IR-780 iodide	Solvothermal (180°C, 24 h)	Filtration (0.22 µm); dialysis	TEM; ~5 nm; UV-vis spectroscopy; PL; XPS; FTIR; DLS	Ultrasound-assisted tumor ablation	Jana e <i>t al.</i> ., 2021
Rhodamine B, H_2O_2 , and ethanol	Solvothermal (200°C, 20 h)	Dialysis	HRTEM and TEM; 1.5–6 nm; UV-vis spectroscopy; PL; XPS; FTIR; Raman; AFM	Anti-counterfeiting and bioimaging	Shi <i>et al.</i> , 2023

Dodecylamine and chlorobenzene	Reflux (48 h)	Silica gel column chromatography	TEM; 3 nm; UV-vis spectroscopy; PL; XPS; FTIR; XRD; Raman; ¹H-NMR, and ¹³C-NMR	Fluorescent inks	Yin <i>et al.</i> , 2019
Melamine, dithiosalicylic acid, and acetic acid solution	Solvothermal (180°C for 10 h)	Water-wash method, column chromatography	HRTEM and TEM; 6.5 nm; UV-vis spectroscopy; PL; XPS; FTIR; XRD; Raman; 'H-NMR, and '3C-NMR	Reversible two-switch mode luminescence ink	Yang e <i>t al.</i> , 2019
Red wine lees, dodecylamine	Pyrolysis (300°C for 3 h)	Solvent extraction	TEM; 7±3 nm; UV-vis spectroscopy; PL; FTIR	Fluorescent inks	Varisco <i>et al.</i> , 2017
o-Phenylenediamine and pyridinedicrboxylic acid	Pyrolysis (180°C for 4 h)	Water-wash method	TEM; 4.59 nm; UV-vis spectroscopy; PL; XPS; FTIR; XRD; DLS; Raman	Rapid visualization of latent fingerprints	Bandi <i>et al.</i> , 2020
Citric acid and hexadecylamine	Pyrolysis (160°C for 1–5 h)	Filtration (0.2 µm)	HRTEM and TEM; 3.4, 4.6 nm; UV-vis spectroscopy; PL; XPS; FTIR; XRD; WCA; Zeta potential	Liposomes and acrylate films	Fan et al., 2019
Glucose, octadecylamine, octadecene, and chloroform	Hydrothermal (160°C for 30 min)	Solvent extraction; column chromatography	HRTEM and TEM; 3.5 nm; UV-vis spectroscopy; PL 'H-NMR; DLS	Detection of Cu^{2+} in liver cells	Lu <i>et al.</i> , 2017
Ionic liquid (1,3-dibutylimidazolium dicyandiamide, Bbim DCN)	Microwave-assisted (1,300 W for 5 min)	Centrifugation; dialysis	HRTEM; 3.5 nm; UV-vis spectroscopy; PL; XPS; FTIR	Detection of yeast Saccharomyces cerevisiae	Wang e <i>t al.</i> , 2018
Triolein and sulfuric acid	Chemical oxidation	Solvent extraction; centrifugation; dialysis	TEM; 6 nm; UV-vis spectroscopy; PL; XPS; FTIR; Zeta potential	Detection of sodium copper chlorophyllin in nonalcoholic flavored drink	Lin <i>et al.</i> , 2022
5,5'-disulfanediylbis(2-nitrobenzoic acid), ethanol	Solvothermal (180°C for 10 h)	Solvent extraction	TEM; 3 nm; PL	Detection of explosive picric acid in a nonaqueous solution	Pagidi <i>et al.</i> , 2022
Maleic acid and oleylamine	Solvothermal (180°C for 6 h)	Solvent extraction	HRTEM and TEM; 60 nm; UV-vis spectroscopy; PL; XPS; FTIR; XRD	Detection of nitroaromatic compounds	Garg <i>et al.</i> , 2022
Citric acid, acidified solution of methionine	Thermal process (300°C for 30 min)	Solvent extraction; centrifugation; dialysis	TEM; <4 nm; UV-vis spectroscopy; PL; Zeta potential; XPS; FTIR	Detection of Al³* and intracellular imaging of Al³*	Kong <i>et al.</i> , 2017
L-ascorbic acid and oleylamine	Solvothermal (200°C for 4 h)	Solvent extraction; centrifugation	TEM; ~3.5 nm; UV-vis spectroscopy; PL	pH-sensor and sodium detection	Galyean <i>et al.</i> , 2018
para Benzoquinone, L-cysteine, ethanol	Microwave (600 W for 10 min)	Dialysis	HRTEM and TEM; 2.7 nm; UV-vis spectroscopy; PL; XPS; FTIR	Moisture sensing	Arshad and Sk, 2019
Cyclohexane	Solvothermal		TEM; ~3.5 nm; UV-vis spectroscopy; PL; XPS; FTIR; ¹3C-NMR; SAED	Selective sensing of 2,4,6-trinitrophenol	Ganiga <i>et al.</i> , 2018
Ascorbic acid, hexadecylamine, and absolute ethanol	Reflux (8 h)	Solvent extraction	HRTEM; 2.1 nm; UV-vis spectroscopy; PL; XPS; FTIR; AFM	Determination of 2,4,6-trinitrophenol	Cheng <i>et al.</i> , 2015
Citric acid, methyl amine, n-butyl amine, and n-octyl amine	Solvothermal (180°C for 10 h)	Filtration (0.05 µm), dialysis	TEM; 2.0–4.0 nm; UV-vis spectroscopy; PL; XPS; FTIR; Zeta potential	Selective detection of nitroexplosive	Mondal <i>et al.</i> ., 2023
D-phenylalanine and toluene	Hydrothermal (240°C for 14 h)	Solvent extraction	HRTEM and TEM; 2.5 nm; UV-vis spectroscopy; PL; XPS; FTIR; Raman	Detection of nimetazepam	Yen et al., 2020
					(continues)

Table 1. Continued.					
Precursors	Synthesis method	Extraction/purification	Method of characterization	Application	Reference
Tea saponin and hydrochloric acid	Solvothermal (230°C for 6 h)	Silica gel column chromatography	HRTEM and TEM; 2.5 nm; UV-vis spectroscopy; PL; XPS; FTIR; XRD; Zeta potential	Detection of HSA and extremely acidic pH, bioimaging	Zhang et al., 2023a
Methylene blue, sulfuric acid, ethanol	Solvothermal (200°C for 6 h)	Filtration (0.22 µm)	HRTEM and TEM; 9 nm; UV-vis spectroscopy; PL; XPS; FTIR; XRD; AFM; Raman	Detection of Au ³⁺ Cell imaging Fabrication of white-LEDs	Gao <i>et al.</i> , 2019
Citric acid and L-tyrosine	Solvothermal (220–300°C for 30 min)	Filtration	TEM; <4 nm; UV-vis spectroscopy; PL; XPS; FTIR; ¹H-NMR, ¹³C-NMR	Ethoxide ions and Ag NPs detection	Gude, 2014
Octadecylamine, glucose, ethanol	Refluxing (8 h)		TEM; 5.4 nm; FTIR; XPS; WCA	Chromatographic stationary phase	Chen <i>et al.</i> , 2021b
Citric acid, octadecanamine, 1-aminoethyl-3-methylimidazolium bromide, ethanol	Hydrothermal (180°C for 4 h)	Dialysis	TEM; 3.2 nm; XRD; FTIR	Multi-mode HPLC	Yang <i>et al.</i> , 2022
Choline chloride and lactic acid	Hydrothermal (180°C for 4 h)	Dialysis	TEM; 3.2 nm; FTIR; DLS; EDS; Zeta potential; WCA	Chromatographic stationary phase	Fu <i>et al.</i> , 2022a
Choline chloride, lactic acid, and phosphoric acid	Hydrothermal (180°C for 4 h)	Dialysis	TEM; 3.1 nm; FTIR; DLS; EDS	Mixed-mode stationary phase	Fu <i>et al.</i> , 2022b
Melamine, urea, sulfonamide, dithiosalicylic acid, and acetic acid	Solvothermal (180°C for 10 h)	Water-wash method; centrifugation	HRTEM and TEM; 2–7 nm; UV-vis spectroscopy; PL; XPS; FTIR; XRD; Raman	LEDs and fingerprints applications	Xu <i>et al.</i> , 2023
Oil-soluble 1,3,6-trinitropyrene and toluene	Solvothermal (180°C for 12 h)	Filtration (through 0.22 µm)	HRTEM and TEM; 2.6 nm; UV-vis spectroscopy; PL; XPS; FTIR; XRD; Raman	Phosphor-based LED lamp	Wu <i>et al.</i> , 2017
L-cysteine hydrochloride anhydrous, citric acid, and dicyclohexylcarbodiimide	Solid-phase route (180°C for 40 min)	Solvent extraction; dialysis	TEM; 5.8 nm; UV-vis spectroscopy; PL; XPS; FTIR	LED lamp production and solid fluorescent shaping material	Zhao <i>et al.</i> , 2020
Urea, citric acid, DMF, NaOH/KOH	Solvothermal (160°C for 6 h)	Centrifugation	HRTEM and TEM; 4–10 nm; UV-vis spectroscopy; PL; FTIR; EDX; AFM; Zeta potential	White LEDs	Qu <i>et al.</i> , 2016
Ammonium bicarbonate, (NH₄HCO₃), acetic acid, toluene, octadecylamine	Solvothermal (160°C for 4 h)	Solvent extraction; centrifugation	HRTEM and TEM; <5 nm; UV-vis spectroscopy; PL; XPS; FTIR	Transparent fluorescent bulks	Chen <i>et al.</i> , 2015
Candle soot, styrene	Flame synthesis	Solvent extraction; centrifugation	TEM; 2–5 nm; UV-vis spectroscopy; PL; FTIR; DLS; Zeta potential Raman	Labeled microplastics	Shebeeb <i>et al.</i> , 2022
Urea, citric acid, oleylamine, toluene	Refluxing (130°C for 6 h)	Centrifugation; dialysis	TEM ;4–12 nm; UV-vis spectroscopy; PL; XPS; FTIR; XRD; Raman	Lubrication test	Shang <i>et al.</i> , 2018

Cetylpyridinium chloride monohydrate, NaOH	Chemical oxidation	Solvent extraction; vacuum drying	HRTEM; FESEM; UV-vis spectroscopy; XPS; FTIR; Raman; WCA	lodine adsorption in water	Zheng <i>et al.</i> , 2019
Acetaldehyde, sodium hydroxide	Chemical carbonization	Centrifugation	TEM; 3–5 nm; UV-vis spectroscopy; PL; FTIR; SAXS	Forward osmosis membrane	Zhang <i>et al.</i> , 2021
Melamine, dithiosalicylic acid, acetic acid	Hydrothermal (180°C for 10 h)	Water-wash method; vacuum filtration	TEM; 0.8–7 nm; UV-vis spectroscopy; PL; XPS; FTIR; XRD; Raman	Monitoring seafood freshness	Zhang <i>et al.</i> , 2023b
Calix[4]pyrrole	Hydrothermal (200°C for 8 h)	Centrifugation; filtration	HRTEM and TEM; 4–10 nm; UV-vis spectroscopy; PL; XPS; FTIR; XRD	Solar cell	Coşkun <i>et al.</i> , 2022
Cetylpyridinium chloride monohydrate, NaOH, HCI	Chemical oxidation	Solvent extraction; dialysis	TEM; 2 nm; FTIR; WCA	Self-cleaning and anti-corrosion	Marković <i>et al.</i> , 2022

transform infrared spectroscopy); HRTEM TEM (High-resolution transmission electron microscope); LED (light-emitting diodes); NMR (Nuclear magnetic resonance); SAED (Selected area electron diffraction); AFM (Atomic force microscopy); CDs (Carbon dots); DMF (Dimethylformamide); DLS (Dynamic light scattering); EDS (Energy dispersive X-ray spectroscopy); HSA (human serum albumin) FTIR (Fourier UV (ultraviolet-visible); WCA (Water contact angle); XRD (X-ray diffraction) gravimetric analysis); I PL(Photoluminescence); SAXS (Small-angle X-ray scattering); TGA (Thermal (5.70 nm) exhibited red emission with a maximum fluorescence wavelength of 650 nm.

Hydrothermal/solvothermal procedure

Hydrothermal/solvothermal procedure involves the use of heat and pressure in sealed containers to treat water-based (hydrothermal) or organic-based (solvothermal) solutions containing different precursors. These methods are used to synthesize various CDs and HCDs by adjusting their temperature, pressure, and reaction period. These methods are simple, cost-effective, and size, shape, and surface can be changed (Dutta and Karak, 2022).

Yang et al. (2019) synthesized dispersed blue-emitting and aggregation-induced red-emitting HCDs by adding melamine and dithiosalicylic acid to an acetic acid solution and using a one-pot solvothermal method at 180°C for 10 h (Figure 2A(a)). As illustrated in Figure 2A(b), the as-synthesized HCDs showed reversible two switchmode luminescence properties, so that the addition of water turned on the red emission of the liquid HCDs, and the addition of ethanol displayed the blue emission of HCDs. In addition, after purifying and drying blue-luminance HCDs, the output of HCD powders emitted red aggregation-induced emission. Recently, Mondal et al. (2023) synthesized HCDs employing a solvothermal method with citric acid as a carbon source, subsequently subjecting them to surface functionalization with alkylamines possessing diverse hydrophobic alkyl chains (methyl amine, n-butyl amine, and n-octyl amine). They ascertained that the solubility of CDs was elevated in aqueous media in comparison to organic solvents. Moreover, butyl-amine-functionalized CDs exhibited solubility in both polar and nonpolar media because of the co-presence of hydrophilic and hydrophobic functional groups on the surfaces of CDs whereas octyl amine-functionalized CDs demonstrated solubility exclusively in organic solvents. Similarly, riboflavin is carbonized into HCDs in the presence of ethylenediamine and acetone (Marković et al., 2022). For this purpose, riboflavin was first dissolved in acetone, and ethylamine was added dropwise to obtain a transparent dark orange solution and heated at 180°C for 12 h. In another study, highly luminescent HCDs were synthesized using a hydrothermal technique (Coşkun et al., 2022). The carbon precursors were calix[4]pyrrole and n-hexane, separately dissolved in toluene, and heated at 200°C for 8 h (Figure 2B). Results demonstrated that HCDs in toluene exhibited a smooth crystalline structure and high stability.

Other environmentally sustainable carbon sources, such as biomass, biowastes, and other carbon precursors, are explored by researchers for the synthesis of various

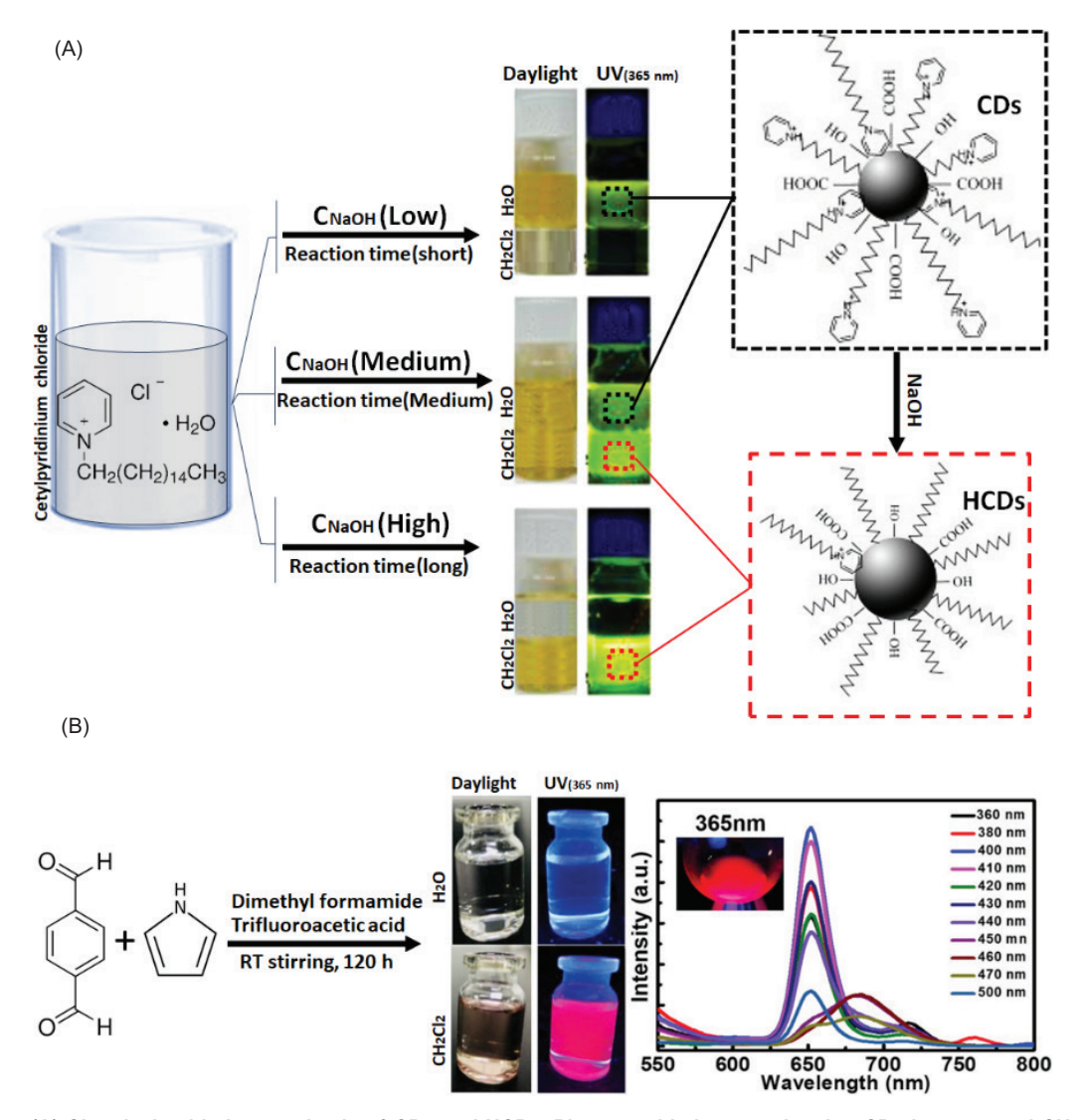


Figure 1. (A) Chemical oxidation synthesis of CDs and HCDs. Photographic images showing CDs in water and CH₂Cl₂ under daylight and ultraviolet (UV) light (at 365 nm) (adapted from Zheng *et al.*, 2015); (B) schematic of chemical oxidation approach to HCD synthesis from pyrrole and terephthalaldehyde, trifluoroacetic, and DMF. Photos of HCDs in daylight and UV light, and fluorescence spectra in CH₂Cl₂ (adapted from Feng *et al.*, 2020).

HCDs using hydrothermal methods (Ndlwana et al., 2021). For example, fluorescent HCDs are synthesized hydrothermally using Clitoria ternatea leaves. The ethanolic extract of the plant was first prepared and heated at 160°C for 24 h. The crude product was subsequently combined with a mixture of 1:1 dichloromethane:water and the organic layer containing HCDs was collected as the final product (Shinde et al., 2023). Multifunctional HCDs with an average size of 2.5±1 nm with various surface functional groups (OH/NH, C=O, C-N, and C-O-C) were produced using a facile solvothermal method with tea saponin as a precursor (Zhang et al., 2023a). Shi et al. (2023) reported an innovative use of Rhodamine B as a precursor for the hydrothermal synthesis of nearinfrared (NIR)-responsive HCDs. The significance of this starting material lies in its ability to address the issue of rhodamine, a harmful dye pollutant generated by the textile industry while also offering an opportunity to transform waste into valuable materials. During the synthesis process, the organic dye, ethanol, and hydrogen peroxide were heated (200°C for 10 h). The resulting HCDs exhibited tunable excitation wavelengths and upconverted fluorescence within the UV–NIR range.

Pyrolysis treatment

During pyrolysis, the carbon precursors are heated to high temperatures, leading to thermal decomposition. The main advantages of this method are solvent-free nature, short reaction time, cost-effectiveness, ease of performance, and scalability, making it a preferred choice

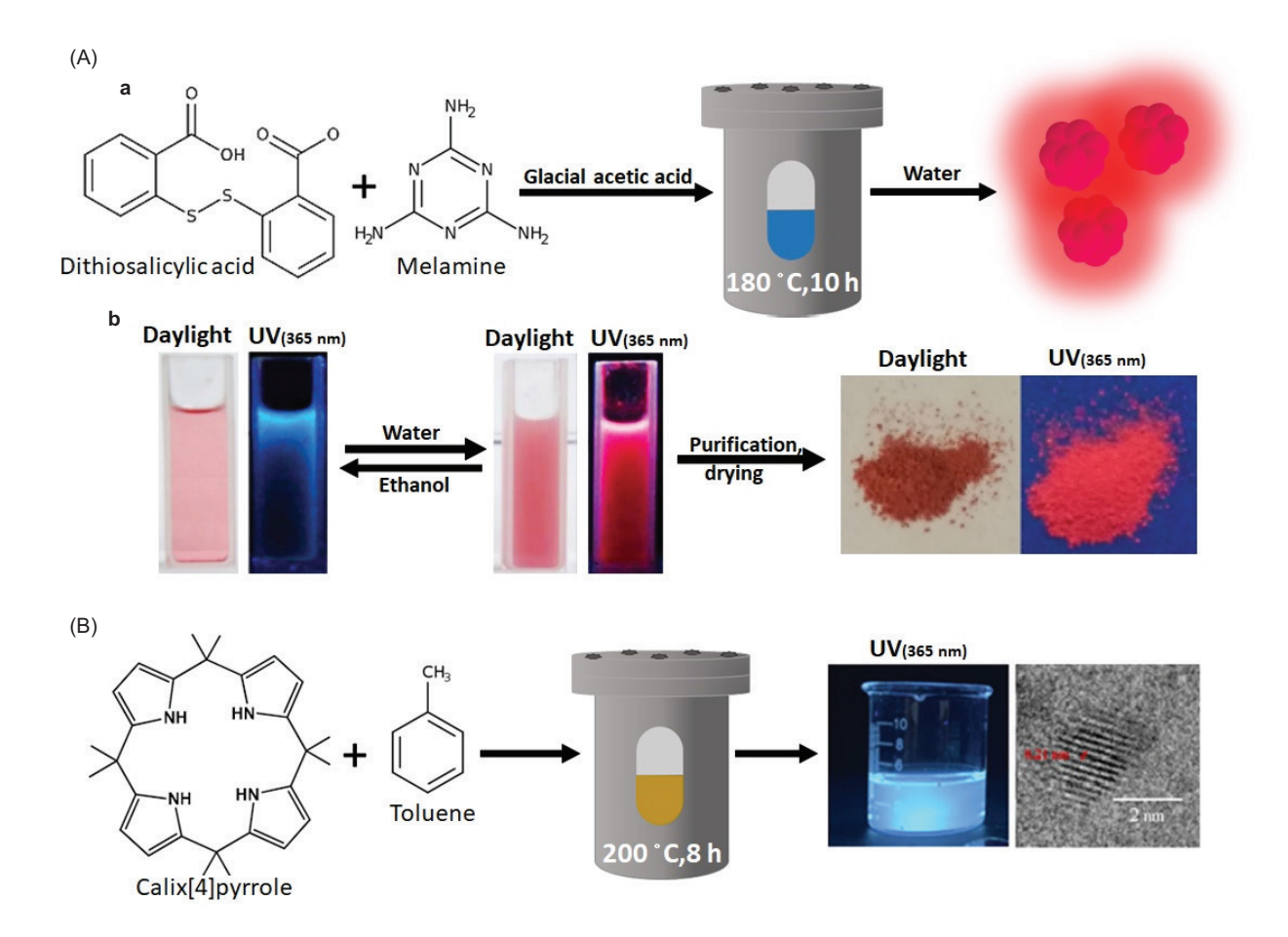


Figure 2. (A) (a) Hydrothermal formation of HCDs; (b) photographs of two-switch-mode luminescence of HCDs in water and re-dissolution in ethanol, and the dried product under sunlight and UV light (365 nm); (adapted from Yang et al., 2019). (B) Synthesis of blue-emitting HCDs from calix[4]pyrrole and the bright blue emission of the prepared HCDs under UV light (366 nm) (adapted from Coşkun et al., 2022).

over the hydrothermal/solvothermal method (Khairol Anuar et al., 2021; Tajik et al., 2020). Various polymeric feedstocks have been explored for pyrolytic HCDs syntheses. For example, Bodik et al. (2018) prepared a mixture of polyoxyethylene-polyoxypropylene-polyoxyethylene triblock copolymer (Pluronic PF-68) and phosphoric acid, which was heated to 250°C with stirring for 2 h to form spheroid shape HCDs (5 nm) (Stanković et al., 2018). Bourlinos et al. (2008) investigated the nonlinear optical response of HCDs synthesized through pyrolysis of lauryl gallate powder. The precursor was placed in a porcelain crucible without any secondary or modifier agents and heated at 270°C for 2 h. The same research group synthesized HCDs through one-step pyrolysis decomposition using various ammonium citrate salts, where the citrate unit and organic ammonium served as the source of carbon cores and surface modifiers, respectively. The results showed that when 2-(2-aminoethoxy)-ethanol citrate salt precursors were used, hydrophilic CDs were synthesized whereas the

carbonization of octadecyl ammonium ($C_{18}H_{37}NH_3^+$) citrate salt resulted in the formation of HCDs. Cheng *et al.* (2015) developed a green method to make fluorescent HCDs using ascorbic acid and hexadecylamine. After sonication, mixing, and refluxing in an oil bath, the obtained mixture was purified using acetone and dried in a vacuum oven to yield the HCD product. The acquired HCDs showed green fluorescence when excited with 365-nm UV radiation. This probe could be used to detect 2,4,6-trinitrophenol in hydrophobic media.

Microwave-assisted

This process allows rapid synthesis of HCDs in the order of a few minutes with high yield. The efficiency and simplicity of this process have attracted the interest of researchers (Li *et al.*, 2021b). For example, Wang *et al.* (2018) prepared HCDs (3.5 nm) in the presence of pyridinic nitrogen, pyrrolic nitrogen, and sp³ hybrid nitrogen

by mixing 1,3-dibutylimidazolium dicyandiamide ionic liquid and ethanol, followed by reaction under microwave irradiation at 1,300 W for 5 min. The ionic liquids with cationic moieties consisting of N-heteroaromatic rings or ammonium derivatives are susceptible to decomposition, thereby greatly improving the efficiency of carbonization.

In another study, Mitra *et al.* (2012) reported a straightforward microwave synthesis of fluorescent HCDs using a domestic microwave oven. To avoid multistep functionalization and expensive raw materials, they used poloxamer Pluronic F-68 and phosphoric acid as precursors and an optimal synthesis process at 450 W for 4 min. Wen *et al.* (2019) developed a microwave-assisted synthesis of monodispersed HCDs (5.5 nm with various surface functional groups) using pheophytin powder dissolved in N,N-dimethylformamide at 500 W for 30 min.

Other methods

Solid-phase synthesis is an alternative approach to HCDs synthesis. This method eliminates the need for strong acids/bases and organic reagents, making it more environment-friendly than other techniques. Zhao et al. (2020) synthesized HCDs utilizing L-cysteine, citric acid, and N,N'-dicyclohexylcarbodiimide (DCC) as precursors in the presence of minimal water. The as-prepared HCDs had excellent PL properties and are useful as a light source in white light-emitting diode (LED) lamps and solid luminescent structures. Talib et al. (2015) developed a novel technique that utilized paraplast granules, which are high-purity polymer blends used in tissue embedding and prosthesis devices, as the precursors. The granules were melted at 70°C and rapidly injected into a toluene solution with gentle stirring while being flushed with nitrogen. Notably, dodecanethiol was added to the reaction mixture to enhance PL and provide surface passivation of HCDs. The mixture was stirred until it developed a yellow-green color. The synthesized HCDs had sizes in the range of 5–30 nm and emitted a strong bright blue fluorescence.

Purification

When synthesizing CDs, impurities, such as molecular intermediates and unreacted substrates, can affect the characteristics of synthesized products, especially their PL and quantum yields. Research indicates that CDs produced through bottom-up methods have higher purity whereas a purification process is necessary for CDs fabricated using top-down routes (González-González et al., 2022). Various purification methods of CDs are reported in the literature, such as washing, centrifugation, filtration, dialysis, ion-exchange chromatography, reversed-phase chromatography, gel electrophoresis, solvent

extraction, and so on (Yao *et al.*, 2019). The water-wash method (boiling water) is commonly used to remove unreacted substrates by adding a reaction mixture to boiling water. The purification efficiency of this technique is comparable to that of column chromatography (Yang *et al.*, 2019).

In contrast, solvent extraction relies on the dispersion of HCDs in hydrophobic or hydrophilic solvents (Cook et al., 2021). Organic solvents, such as chloroform, ethyl acetate, toluene, hexane, carbon tetrachloride, dichloromethane, N-methyl-2-pyrrolidone (NMP), DMF, acetonitrile, and ether, are commonly used to purify synthesized HCDs (Mitra et al., 2012). The effectiveness of the solvent extraction method in separating and purifying HCDs is influenced by the polarity and structural characteristics of the solvent employed. Han et al. (2014) reported a gradient extraction technique involving the use of solvents with varying polarities to extract different fractions of HCDs. The organic solvents used were n-hexane, CHCl₂, and CHCl₂, with respective polarities of 0.06, 1.6, and 3.4. Additionally, a mixture of CHCl₃ and CHCl₂ in a ratio of 3:2 was used. The four extracted fractions exhibited a narrow size distribution, with an average diameter of approximately 3 nm, and a consistent spherical morphology. Furthermore, the intensity of surface functional groups, encompassing polar groups, such as O-H/N-H and C=O, and nonpolar groups, such as C-C, C=C, and C-H, on the as-prepared nanodots demonstrated a direct correlation with the polarity of the solvents utilized during extraction. Specifically, an increase in the polarity of the extraction solvent resulted in a corresponding increase in the number of heteroatoms present on the surface of CDs (Han et al., 2014). For example, after solid-phase synthesis using anhydrous L-cysteine hydrochloride and citric acid, it was found that HCDs could dissolve in commonly used organic reagents (e.g., dimethyl sulfoxide [DMSO], tetrahydrofuran (THF), and various alcohols) with polar coefficients ranging from 7.2 and 3.4. However, their solubility in organic solvents with polar coefficient of less than 3.4 was significantly low (Zhao et al., 2020). Importantly, the PL properties of the extracted CDs were influenced by their respective surface polarities.

However, Yin et al. (2019) synthesized HCDs from aliphatic compounds with a single terminal functional group and performed either gel permeation chromatography or silica gel column chromatography to purify HCDs, resulting in the acquisition of highly pure HCDs with absolute fluorescence quantum yields exceeding 10%. As shown in Figure 3A, the separation of HCDs from 3,4,5-tris(octadecyloxy)benzaldehyde by gel permeation chromatography with toluene as an eluent yielded five fractions of nanodots with different fluorescence properties. Researchers have also explored the purification of

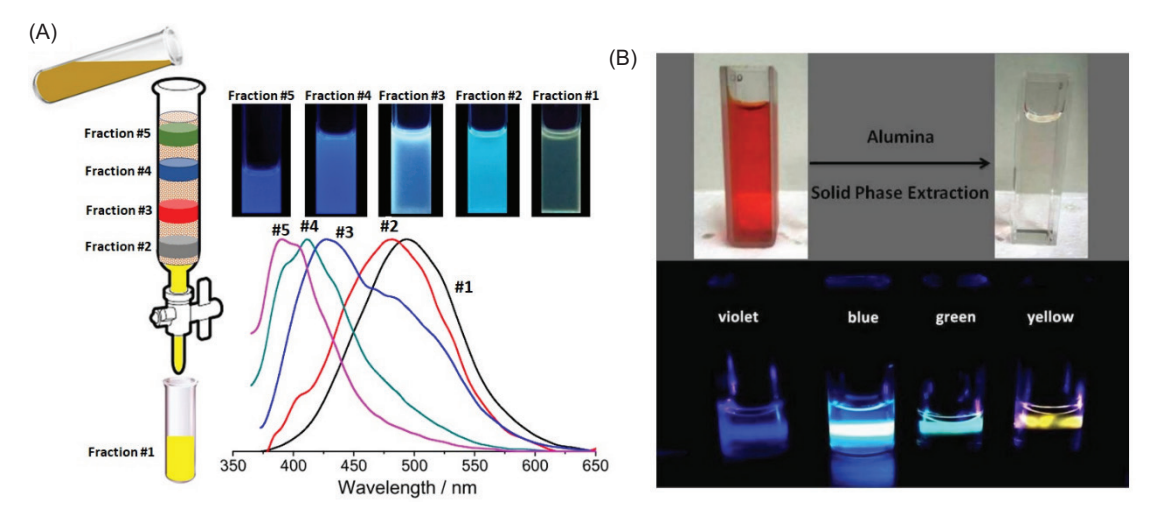


Figure 3. (A) Separation schematic of the synthesized HCDs by gel permeation chromatography, which illustrates the separated fluorescent fractions of the synthesized HCDs from 3,4,5-tris(octadecyloxy)benzaldehyde under 365-nm UV irradiation, and their relevant emission spectra excited at 360 nm (adapted from Yin et al., 2019). (B) Photo of the as-prepared HCDs before (red-brown) and after (colorless) the purification step. Violet-, blue-, green-, and yellow-emitting CDs (when exposed to 365-nm UV radiation) were obtained by eluting the Al₂O₂ column with various solvents (adapted from Koutsioukis et al., 2018).

tea saponin-derived HCDs using silica gel column chromatography, with dichloromethane used as an eluent (Zhang et~al., 2023b). Koutsioukis et~al. (2018) employed a purification technique based on solid-phase extraction of fluorescent CDs by passing the product of hydrothermal synthesis through a tube packed with neutral aluminum oxide (Al $_2$ O $_3$). The HCDs were then retrieved from alumina using appropriate elution solvents. They separated yellow-, blue-, violet-, and green-emitting CDs by eluting the column with ethanol, acetone, and chloroform, respectively (Figure 3B).

In addition, dialysis bag of 100-kDa molecular weight cut-off (MWCO) was used to purify dye-derived HCDs (1.5 to 6 nm) (Shi *et al.*, 2023). In another study, Wang *et al.* (2018) refined HCD solution using a dialysis bag with a 500-Da MWCO in ultrapure water. This process led to a narrow range of particle sizes, averaging around 3.5 nm. Despite its effectiveness, the dialysis method is time-consuming and not suitable for large-scale production. To remove residual acetone and obtain pure HCDs, the remaining supernatant was subjected to centrifugation at $10,000 \times g$ for 10 min. Other researchers reported the removal of impurities from the synthesized HCDs of paraplast granules and riboflavin using a 0.2- μ m filter (Talib *et al.*, 2015) and 100-nm nylon filter membranes (Marković *et al.*, 2022), respectively.

Hydrophobicity Determination of HCDs

In pharmaceutical applications, the hydrophobicity of nanomaterials can affect their pharmacokinetics, host immune responses, bioaccumulation, and toxicity (Taylor et al., 2022). Currently, standardized quantitative procedures for determining the hydrophobicity of nanomaterials do not exist, although some researchers have used the partition coefficient (Kow) as an indicator of hydrophobicity. K_{ow} quantifies a compound's hydrophobicity by comparing its relative distribution between water and n-octanol at a specific temperature (Amézqueta et al., 2020). This two-phase system served as a synthetic reference model, allowing for the evaluation of polarity without significantly altering the properties of either phase. The hydroxyl group in n-octanol functions as both hydrogen-bond donor and acceptor, enabling it to interact with various polar groups. This interaction enhances the solubility of these polar groups within the octanol phase. Additionally, n-octanol possesses acceptable viscosity and low vapor pressure, making it suitable for UV detection in quantitative analysis. If the obtained $K_{ow} > 1$, the substance has higher solubility in organic phases (Moldoveanu and David, 2021). A key limitation of this method is that it is only applicable to nanoparticles that remain stable in octanol. It cannot be used when surfactants are present, which are commonly added to stabilize nanoparticle suspensions, because the surfactant distributes unevenly between phases (Taylor et al., 2022).

The hydrophobicity of CDs can also be assessed by contact angle (CA) measurements. The solution of CDs was then applied to a hydrophilic glass slide. Typically, nanoparticles with a CA $> 90^{\circ}$ are considered hydrophobic. Conversely, lower angle values indicate increased hydrophilicity of particles (Guo *et al.*, 2021). Shi *et al.* (2023) measured the CA value of synthesized dye-derived

HCDs on a silicon wafer greater than 105° (on both sides), which confirmed the good hydrophobicity of the synthesized product. In addition, Mitra *et al.* (2012) reported a CA value of approximately 122° for HCDs synthesized from PF-68 in the presence of *o*-phosphoric acid on a standard hydrophilic glass slide, suggesting the hydrophobic characteristics of the as-prepared nanodots. Despite the importance of characterization and hydrophobicity of CDs to increase the understanding of their behavior for various applications, it appears that CDs' hydrophobicity analysis is largely overlooked in many studies.

Characterization Techniques for HCDs

Carbon dots are characterized by nanometrological techniques based on physical measurements at nanoscale level (de Andrés and Ríos, 2021). Figure 4 summarizes the selected instrumental techniques for the characterization of hydrophobic CDs. Certain physical properties may require the use of multiple techniques for a comprehensive examination. The characterization techniques used in various related reports on the synthesis and application of HCDs are listed in Table 1.

Toxicology of HCDs

The biological effects of nanoscale hydrophobic materials occur through specific interactions with lipophilic cellular components, particularly with the cell membrane.

This interaction can alter the structure, organization, and concentration of membrane proteins, thereby affecting their biological functions (Barnoud et al., 2014; Chisari et al., 2009). Owing to their lipophilic nature, hydrophobic nanoparticles can easily traverse the cell membranes and accumulate within cellular and tissue lipids (Puckowski et al., 2016). The safety or toxicity of CDs depends on their specific physicochemical characteristics, including their size, chemical composition, surface chemistry, and charge. These factors are crucial for determining the overall toxicity of CDs (Guha and Ghosh, 2022; Hardman, 2006; Liu and Tang, 2020). In general, the IC₅₀ value can be used as an indicator of nanomaterial cytotoxicity. In a recent study, Chatterjee et al. (2022) applied the 3-(4,5-dimethylthiazol-2-yl)-2,5-diphenyl tetrazolium bromide (MTT) to assess the cytotoxicity of HCDs in human HEK 293 T (embryonic kidney 293) and HeLa cell lines. The synthesized HCDs derived from sucrose and dodecylamine demonstrated low cytotoxicity, with IC_{50} values of 56 g mL $^{-1}$ and 14 g mL $^{-1}$ in HEK 293 T and HeLa cell lines, respectively. Mao et al. (2016) investigated the cytotoxicity of HCDs (~8.52 nm) and surface functionalized by hydroxyl, secondary amide, and aromatic structure groups, using a standard MTT experiment on different cell lines. The results showed that cell viability remained unchanged after the incubation of tumor cells with 50 µg mL⁻¹ HCDs for 24.

To transform HCDs into hydrophilic nanoparticles, CDs encapsulated in human serum albumin (HCDs-HSA), resulting in excellent stability under a wide pH range and ionic strength (Fahmi *et al.*, 2020). The *in vitro*

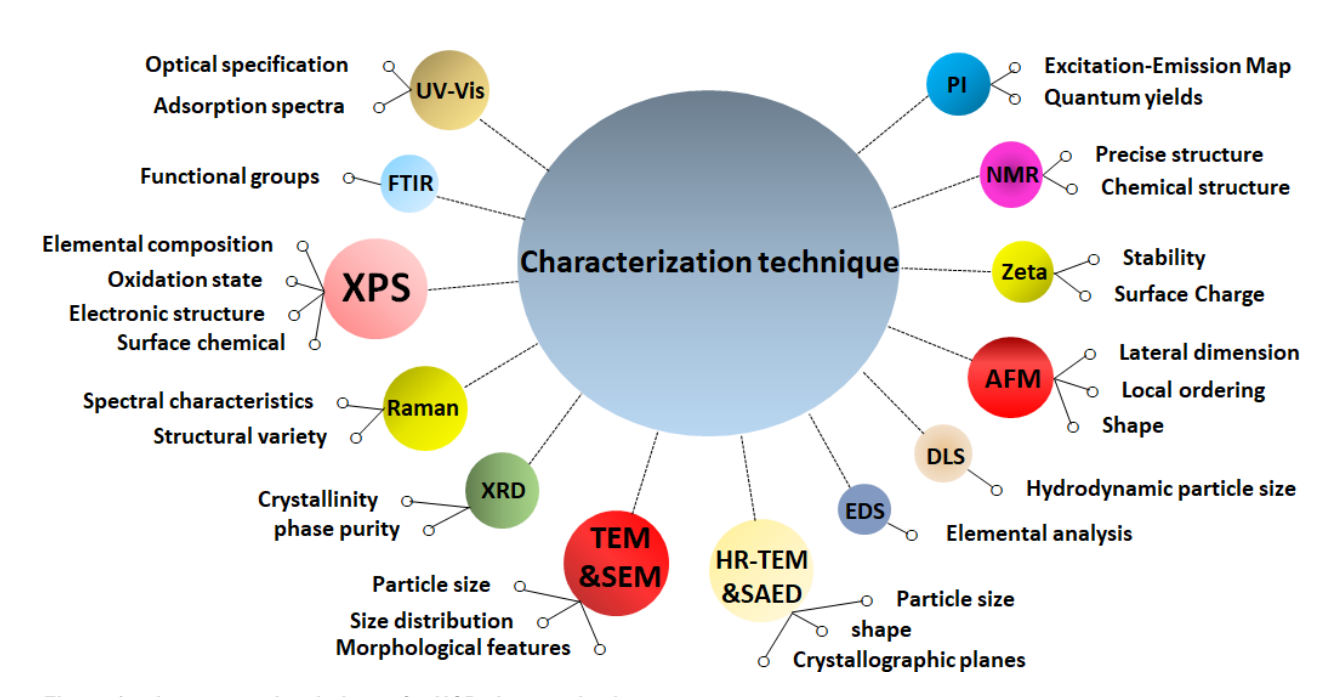


Figure 4. Instrumental techniques for HCD characterization.

cytotoxicity evaluation of HeLa cells using the Cell Counting Kit-8 (CCK-8) assay showed that neither HCDs nor HCDs-HSA caused a significant reduction in the viability of HeLa cells. Moreover, cell viability remained above 80% even at concentrations as high as 500 μg/mL, indicating that both nanoparticles had low cell toxicity. Zhang *et al.* (2023a) used the CCK8 assay to assess the cytotoxicity of HCDs, which were produced from melamine and dithiosalicylic acid, on 293T cells. The results demonstrated that at HCD concentrations of 0.25, 0.5, 1, 2, and 4 mg/mL, cell viability was greater than that of the control group. This suggests that the synthesized HCDs enhanced cell viability and promoted cell growth.

Cytotoxicity is essential when using HCDs for various biological purposes. Choi *et al.* (2018) evaluated the toxicity of HCD probes functionalized with dodecane/sulfobetaine groups on Madin–Darby canine kidney (MDCK) cells and cells isolated from the pleural effusion of a patient with invasive ductal carcinoma (MDA-MB) by using MTT assay. Their results demonstrated that the viability of MDCK and MDA-MB cells remained at or near 100% level at HCDs concentration of up to 0.10 mg. mL⁻¹. Similarly, the MTT assay on HL-7702 cells (Lu *et al.*, 2017) and 4T1 cells (Wen *et al.*, 2019) was also used for

cytotoxicity studies of carbohydrate-derived HCDs and synthesized HCDs from pheophytin, respectively.

In addition to cell lines, other *in vivo* and *in vitro* models are also used by researchers. Zebrafish (*Danio rerio*) embryos were used by Shinde *et al.* (2023) to evaluate HCD toxicity. Embryos were immersed in a suspension of HCDs and collected after different periods of incubation. The distribution of fluorescent dots in zebrafish was assessed using fluorescence microscopy. Their findings verified the absorption and accumulation of HCDs, which did not disrupt the embryos' physiological development or normal growth. This indicates that CDs are biocompatible with *in ovo* zebrafish embryos (Figure 5).

Applications of HCDs

Hydrophobic carbon dots possess fluorescence, photoluminescence, and functional properties that can be exploited for various applications, such as sensing, microbial control, bio-imaging, drug delivery, and electronics (Sun *et al.*, 2022; Yang *et al.*, 2016). In the following sections, the selected HCD applications for food safety and analysis are discussed.

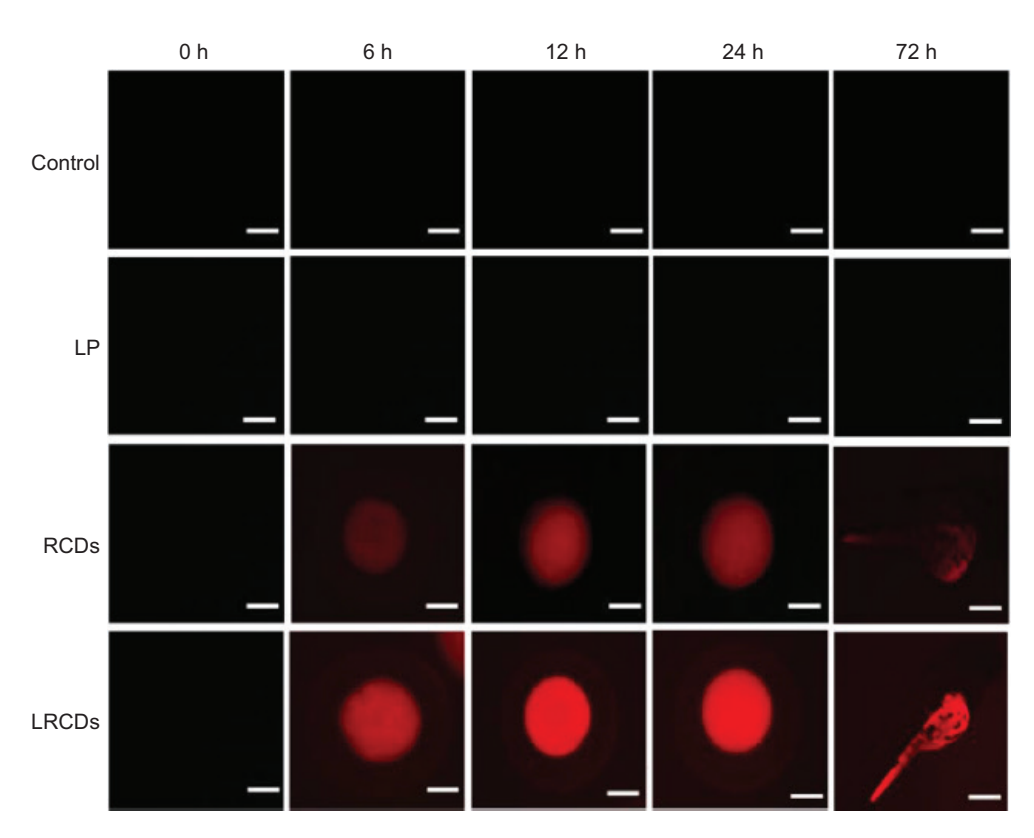


Figure 5. *In ovo* application of CDs in bioimaging studies. (a) Control, liposome (LP), red fluorescent carbon dot (RCDs), and lipid-coated red fluorescent carbon dot (LRCDs) uptake in zebrafish embryos at 0-, 6-, 12-, 24-, and 72-h intervals. (Scale bar: 100 µm) (adapted from Shinde *et al.*, 2023).

Sensor application

Carbon dots possess excellent fluorescence properties and exceptional photostability, making them ideal for use in precise and responsive sensing systems. Several chemical nanosensors based on HCDs are reported. For instance, Cheng et al. (2015) examined the efficiency of HCDs synthesized from vitamin C and hexadecylamine as nanosensors to detect 2,4,6-trinitrophenol (TNP) (a harmful nitroaromatic pollutant nitroaromatic) in hydrophobic media (Figure 6A). The HCDs dissolved in tetrahydrofuran exhibited a strong emission at λ_{em} = 495 nm if excited at λ_{ex} = 410 nm. Upon the addition of 1–110-μM TNP, the fluorescence intensity was quenched linearly (limit of detection [LOD] = 1.8 µM) because of the inner filter effect (IFE) quenching mechanism (Figure 6B). In addition, Figure 6C reveals the responses of portable fluorescent test strips (silica gel TLC plate) under 365-nm UV light without any treatment and after treatment with TNP concentrations of 2, 20, 200, and 400 µM.

An HCD-based fluorescent nanoprobe was developed by refluxing maleic acid and oleylamine, with long-chain oleylamine serving as a self-surface passivating agent for selective sensing of TNP and 2,4-dinitrophenol (DNP) (Garg *et al.*, 2022). The obtained nanodots exhibited excitation-dependent fluorescence properties ($\lambda_{\rm em} = 465$ nm at $\lambda_{\rm ex} = 360$ nm), and these emission intensities were selectively quenched by the addition of TNP and DNP. In that study, the quenching mechanism of the fluorescent nanoprobe was explained using a combination of fluorescence resonance energy transfer (FRET) and photo-induced electron transfer (PET) processes.

Hydrophobic carbon dots-based probes are developed for ratiometric fluorescent sensing of Cu2+ (Lu et al., 2017). To prepare the probe, researchers prepared HCDs, which were derived from glucose, octadecylamine, or octadecene, and then encapsulated in the amphiphilic polymer 1,2-distearoyl-sn-glycero-3phosphoethanolamine-poly(ethylene glycol) (DSPEand tetrakis (4-carboxyphenyl) porphyrin (TCPP)-modified DSPE-PEG through self-assembly. When excited at a wavelength of 405 nm, these structures displayed emissions at 485 nm for HCDs and 655 nm for TCPP. As illustrated in Figure 7, Cu²⁺ ions interact with the

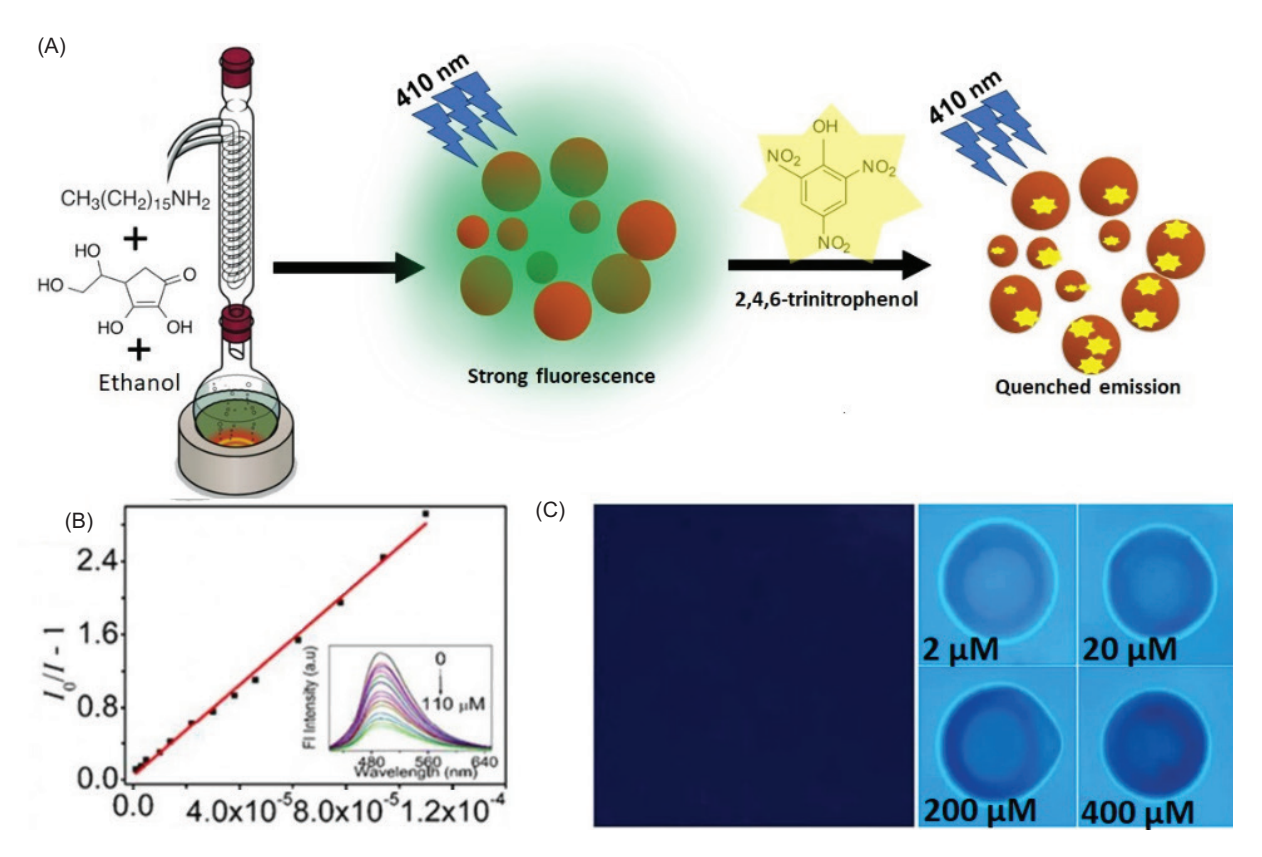


Figure 6. (A) Schematic of HCD synthesis from vitamin C and hexadecylamine and their sensing of TNP; (B) linear relationship between $((I_0/I) - 1)$ and TNP concentration. Emission spectra of the HCDs excited at 410 nm in the presence of different concentrations of TNP (inset); (C) portable fluorescent test strips (silica gel TLC plate) under 365-nm UV light without any treatment and after treatment with various concentrations of TNP (adapted from Cheng et al., 2015).

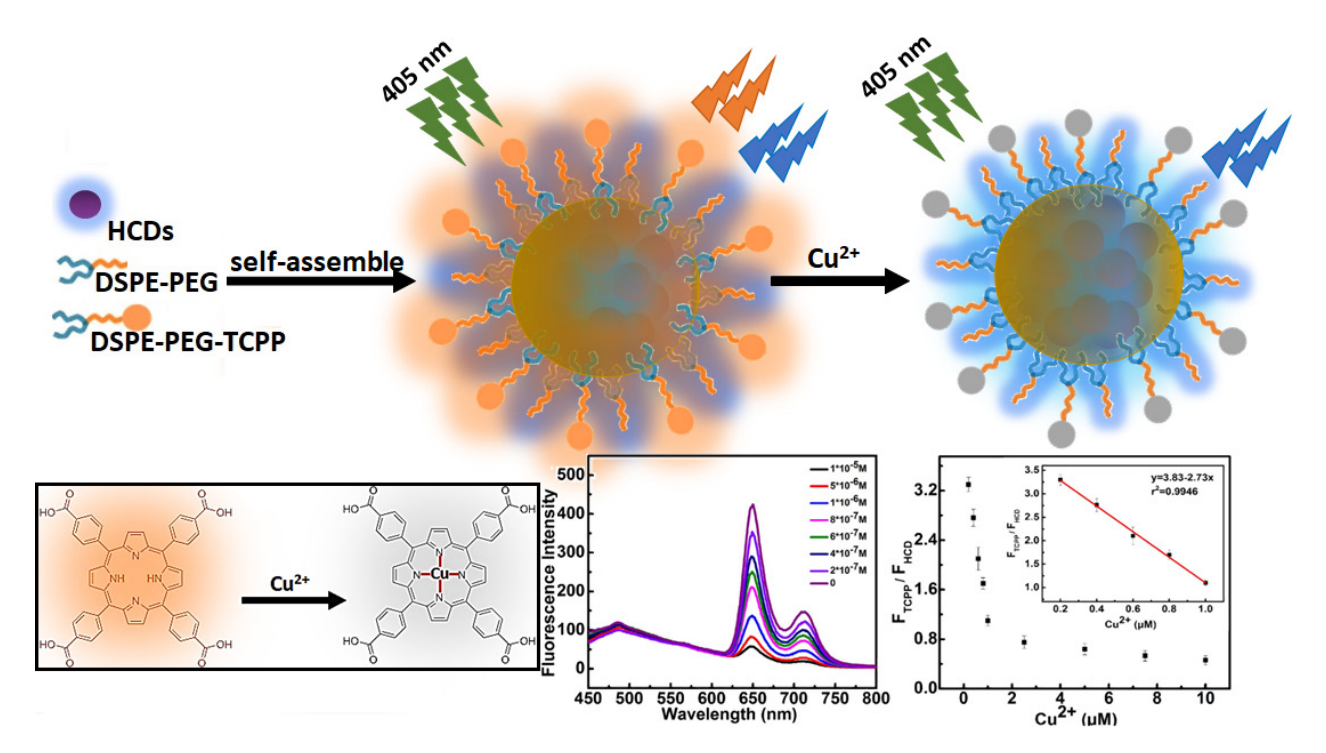


Figure 7. Diagram of HCDs encapsulated in micelles, showing dual fluorescence emissions under a single excitation wavelength (405 nm), quenching mechanism, alterations in the fluorescence spectra of the dual-emission probe when exposed to varying Cu²⁺ concentrations, and the fitting curve of FTCPP/FHCD against different Cu²⁺ levels (adapted from Lu *et al.*, 2017).

nitrogen atom in the porphyrin ring of TCPP, leading to a selective suppression of its fluorescence. For this probe, the plot of the ratio of fluorescence intensity at 655 nm to fluorescence at 485 nm (F.I $_{\rm 655}$ nm/F. I $_{\rm 485}$ nm) versus Cu $^{2+}$ concentration was linear in the range of $2\times10^{-7}-1\times10^{-6}$ M.

In another study, triolein-derived HCDs (TO-HCDs) were developed to detect sodium copper chlorophyllin in nonalcoholic beverages (Lin et al., 2022). The coordination of Cu²⁺ to the surface sulfonyl groups of TO-HCDs induced nanoparticle aggregation, thus causing fluorescence quenching (PET). Practical investigations revealed that TO-CDs are promising for the rapid and accurate detection of Cu2+ ions and copper-based compounds in environmental and food samples (Lin et al., 2022). In addition, Kong et al. (2017) developed HCDs by thermal oxidation of citric acid and methionine, followed by surface modification of HCDs with a long-chain cationic CTAB surfactant through an ion exchange process. They observed that the blue fluorescence emitted by CDs was completely quenched when flavanol and morin molecules bonded to the surface groups of the CDs. With the introduction of Al3+, the fluorescence intensity of the metal-ion complex (MR-Al3+) increased linearly between 8 mM and 20 mM. This HCD-based detection technique enables the quick identification (around 0.5 minutes) of Al3+ in human umbilical vein endothelial cells (Kong et al., 2017).

A new fluorescent sensing platform using HCDs was recently created for detecting HSA. This platform offers a linear detection range of 0–180 μM and is effective across a pH range of 2 to 13 (Zhang et al., 2023). Researchers have reported that when HSA was added to saponinderived HCDs, the fluorescence intensity (at λ_{ox} = 380 nm) increased significantly, reaching up to 6.5 times the original intensity of the as-prepared HCDs. This enhancement was attributed to the decreased polarity of the solvent, which inhibited the rotation or vibration of fluorophore. The LOD for HSA was achieved at a concentration of 140 nM. Additionally, this study revealed that the fluorescence intensity of synthesized HCDs exhibited significant variations under extremely acidic conditions when excited at a wavelength of 380 nm. This result led to the introduction of a sensitive ratiometric pH-detection probe for extremely acidic conditions.

Hydrophobic carbon dots have gained considerable interest in the detection of specific contaminants in food, and Yen *et al.* (2020) designed a highly selective and sensitive detection kit for nitro-substituted benzo-diazepines in beverages, using the fluorescence quenching properties of HCDs. These HCDs were synthesized from d-phenylalanine through a hydrothermal process and exhibited excitation-dependent fluorescence behavior ($\lambda_{\rm em} = 430$ nm at $\lambda_{\rm ex} = 365$ nm) and different quantum yields in toluene, ethyl acetate, and dichloromethane

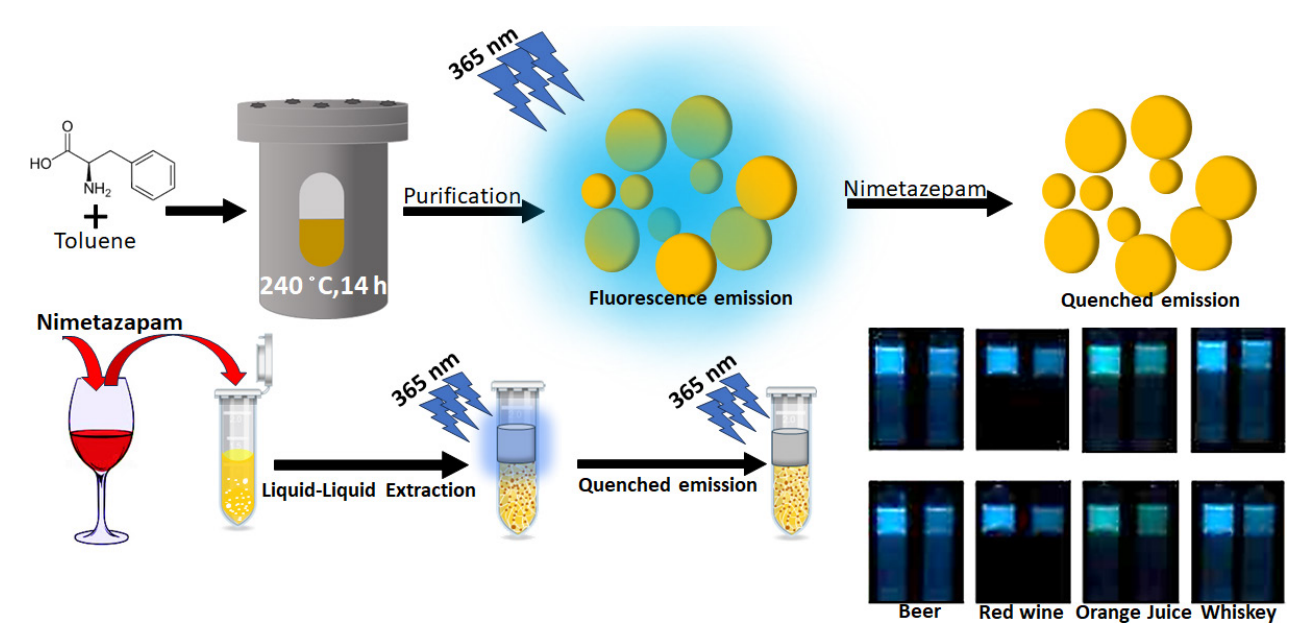


Figure 8. Synthesis and application of as-prepared HCDs from D-phenylalanine for fluorescence sensing of nimetazepam in various beverages (adapted from Yen et al., 2020).

(16.2%, 9.8%, and 9.4%, respectively). The results verified that the analyte caused fluorescence quenching for nimetazepam up to a concentration of 7.24 μ M, with a detection time of <5 min. The assay method was evaluated for the detection of nimetazepam in various beverages, such as beer, red wine, whiskey, and orange juice. Figure 8 shows the concept and application of the proposed probe for determining nimetazepam in some drink samples.

In chemical and industrial applications, accurate monitoring of water content is crucial, as even small amount of water impurities in organic solvents can lead to hydrolysis, generate unwanted oxidation products during processes, or contaminate solvents during storage. Therefore, in one study, the efficiency of a fluorescent probe based on HCDs synthesized via a hydrothermal method from pentafluorobenzyl alcohol in DMF was used to detect water content in DMF (Zhang et al., 2024). In the proposed design, for increasing water content from 2% to 90% (v/v), the PL of HCDs decreased gradually. They examined the effect of fluorescence quenching by observing variations in PL intensity with change in water content, revealing a linear correlation ($R^2 = \sim 0.994$) in broad water content (4–80%). The LOD in DMF was 0.08%, which is considerably lower than the values reported in earlier studies.

Recently, Wang *et al.* (2024) developed a fast, sensitive, and portable sensing platform for detecting ethanol in alcoholic beverages (specifically Chinese Baijiu) using a dual-mode approach that combines optical detection

and smartphone imaging with HCDs. The HCDs, which exhibited bright red fluorescence, were synthesized through a hydrothermal method using o-phenylenediamine, p-aminobenzoic acid, manganese chloride, and hydrochloric acid. The authors found that adding ultrapure water to an ethanol solution containing HCDs led to HCD accumulation, resulting in notable changes in both fluorescence intensity and absorption. Additionally, the color of HCDs in the water-ethanol mixture changed visibly under both daylight and UV light, allowing the creation of a smartphone-based colorimetric detection system for simple and real-time ethanol monitoring. Figure 9 provides a schematic representation of the synthesis process and the ethanol detection mechanism of HCDs. In this approach, captured images of probes exposed to visible and UV light were carefully analyzed, and R, G, and B values were determined. Finally, the linear correlation between ethanol concentration and R, G, and B values was determined. The analytical results indicated that the sensor demonstrated strong sensitivity, a broad detection range, and impressive resistance to interference. Additionally, high recovery rates (96.5-104.5%) and excellent reproducibility (with reproducibility standard deviation [RSDs] < 6.6%) validated its effectiveness for analyzing real samples.

He *et al.* (2024) developed a highly selective fluorometric probe for the specific detection of curcumin using HCDs synthesized from flaxseed oil through a solvent-free reaction. The resulting HCDs emitted blue fluorescence at 425 nm, achieving a relatively high quantum yield of 21.1%. In the presence of curcumin, the fluorescence

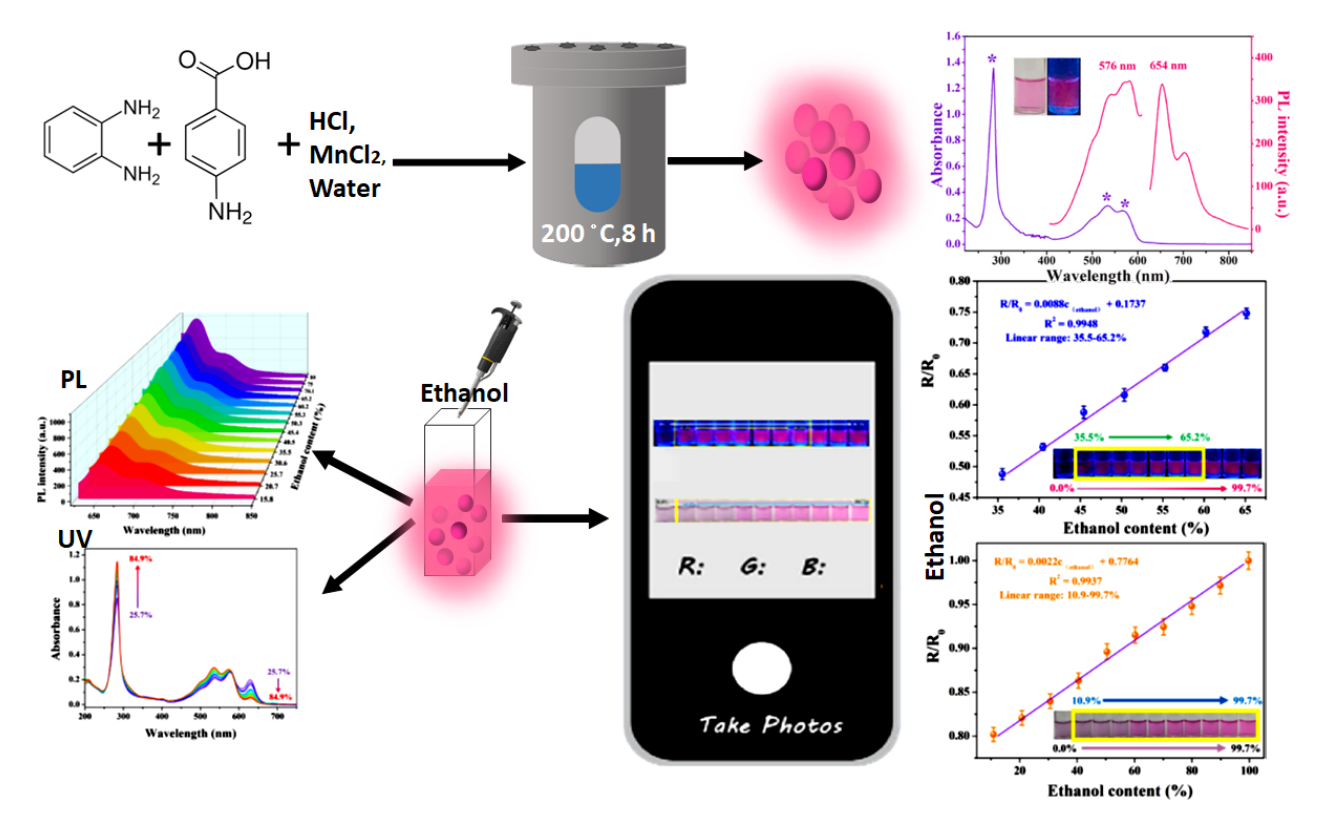


Figure 9. Schematic illustration of HCDs preparation process, PL excitation, PL emission, ultraviolet-visible (UV-vis) absorption spectra of HCDs, and optical dual-mode and smartphone imaging ethanol detection sensor operation (adapted from Wang et al., 2024).

was quantitatively quenched. They proposed that both dynamic and static quenching mechanisms contributed to the probe's signal and found that the sensing HCDs could quickly recover from the tested solutions via solvent-change precipitation. According to their findings, the detection limit for curcumin using this fluorescent method was 20 nM, with a linear response range of 0.2–200 μM . The probe also effectively analyzed various real food samples, including turmeric sugar, curry powder, turmeric powder solid beverage, turmeric milk powder, and ginger powder, yielding reproducible and accurate results.

Galyean *et al.* (2018) also addressed the challenges of using toxic organic dyes or heavy-metal quantum dots incorporating fluorescence HCDs in the ionophore-based optical sodium nanosensor. In their approach, HCDs synthesized from L-ascorbic acid and oleamine, combined with blueberry dye, an ionophore, and a charge-balancing additive, were integrated into an ionophore-based Na⁺ nanosensor. Owing to the interaction between the blueberry dye and HCDs, only the dye becomes protonated at low concentrations of Na⁺, leaving the fluorescence of the HCDs unaffected. As the concentration of Na⁺ rises, the cations engage with the ion-selective receptor at the core of the nanosensor (Figure 10). At the same time,

to preserve the internal charge balance, the dye underwent deprotonation, resulting in a reduction of fluorescence signal from HCDs. The energy transfer mechanism between the dye and HCDs has been suggested to involve FRET or IFE (Galyean *et al.*, 2018).

The emergence of aggregation-induced emission (AIE) approach has provided new insights into the fabrication of fluorescent probes based on CDs. For instance, a ratiometric fluorescent marker utilizes dual-emissive HCDs enables *in situ*, real-time visual evaluation of shrimp freshness (Zhang *et al.*, 2023b). They fixed the HCDs onto a substrate made of cotton fiber paper. The as-prepared tag was used for the visual recognition of volatile base nitrogen (VBNs) using spermine and ammonium hydroxide as typical targets, which displayed distinct color variations from red to blue under UV light (Figure 11). The confirmed mechanism for naked-eye monitoring was based on the disaggregation of HCD aggregates in the presence of VBNs.

Application of HCDs in chromatography

Carbon dots are promising materials for modifying stationary phases in chromatographic applications because

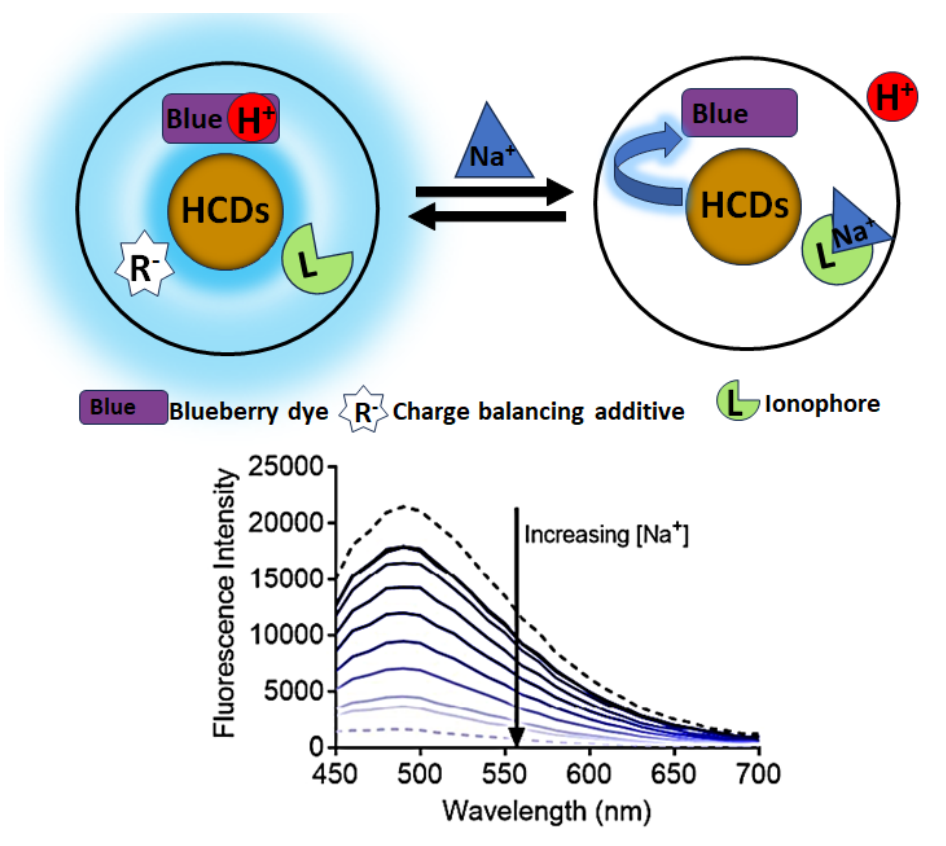


Figure 10. Illustration of the components of HCD nanosensors integrated into the nanosensor matrix, the mechanism of fluorescence quenching, and emission response with increase in sodium (Na⁺) concentrations (adapted from Galyean et al., 2018).

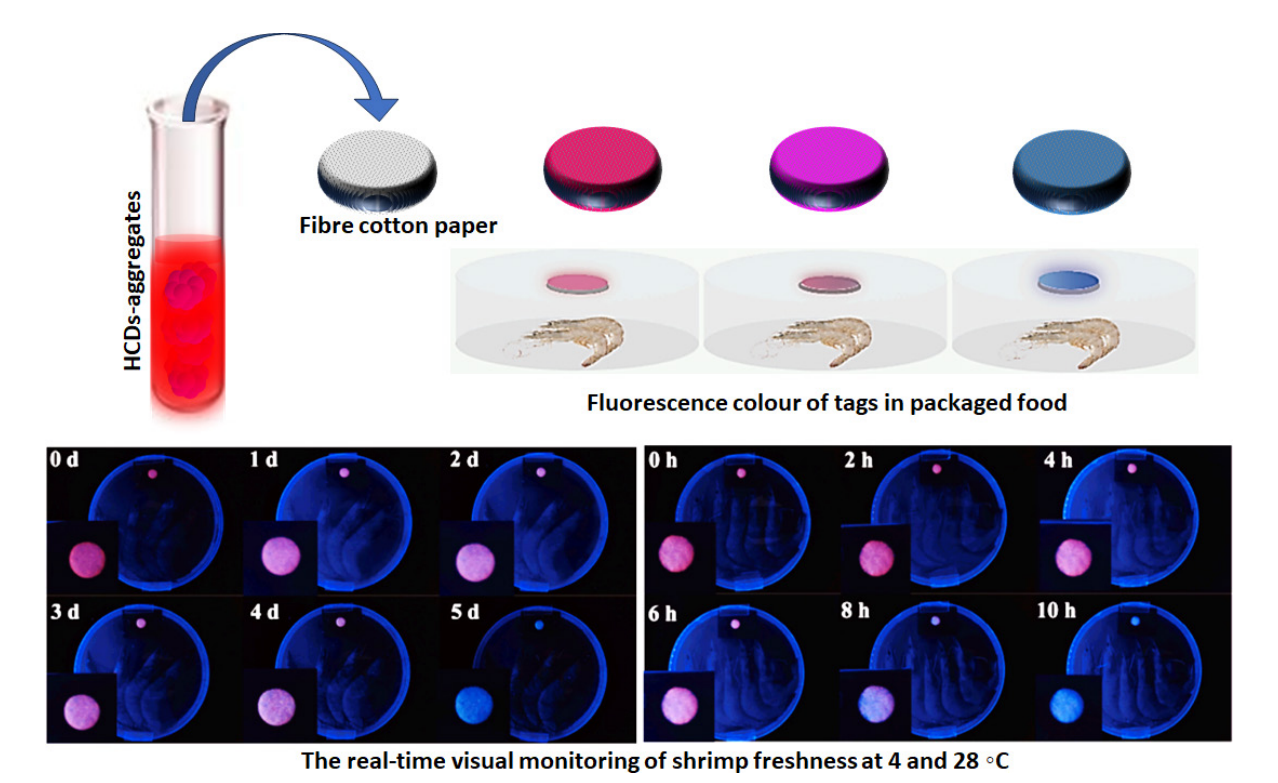


Figure 11. Schematic representation of the preparation process of the loaded HCD aggregates tag and the monitoring of shrimp freshness using this tag at 4°C (left) and 28°C (right). The image includes photographs of the tag after being exposed to shrimp under UV light (adapted from Zhang et al., 2023).

of their nanoscale size, customizable surface chemistry, and moderate adsorption capabilities (Chen et al., 2021a). Fu et al. (2022a) explored the applications of HCDs in chromatography by introducing a novel hydrophobic stationary phase for high performance liquid chromatography (HPLC). The stationary phase was prepared by chemically bonding the deep eutectic solvent-based HCDs to the surface of silica, which was then packed into a stainless-steel column. Tanaka and Engelhardt standard test mixtures were employed to assess the retention behavior of the fabricated stationary phase, including polycyclic aromatic hydrocarbons, flavonoids, aromatic amines, phenolic compounds, and even structurally similar compounds, such as prednisolone and hydrocortisone. The same research group enhanced the separation performance of the chromatographic stationary phase by introducing a mixed-mode approach: reversed-phase and hydrophilic interaction chromatographic modes (Fu et al., 2022b). This was achieved by developing a modified silica stationary phase using phosphorous-doped HCDs synthesized using choline chloride, lactic acid, and phosphoric acid as modifiers to impart specific hydrophobicity, hydrogen-bonding ability, and molecular-shape selectivity for the effective separation of diverse hydrophilic and hydrophobic compounds (Fu et al., 2022b). Jiang et al. (2021) employed an ionic liquid (1-vinyl-3-octadecyl; imidazolium bromide) for the hydrothermal synthesis of HCDs. The prepared HCDs were then grafted and co-grafted onto silica beads for use as stationary phases in the packed HPLC columns. The column's retention characteristics for different hydrophobic compounds (such as Tanaka, Engelhardt, SRM869b, and SRM870) were explained by the π - π interactions occurring between the imidazolium groups on the surface of the HCDs and the analytes. This column demonstrated enhanced selectivity for the separation of isomers of tetracyclic/tricyclic polycyclic aromatic hydrocarbons and butylbenzene when compared to standard C18 columns available on the market.

In a different study, HCDs were synthesized using citric acid, 1-aminoethyl-3-methylimidazolium bromide ionic liquid, and octadecylamine, resulting in multiple surface functional groups, such as carboxyl, amino, hydroxyl, and imidazole groups (Yang *et al.*, 2022). The silica gel bead stationary phase was then modified with the synthesized HCDs with (3-aminopropyl)triethoxysilane as a spacer. The HCD synthesis process, modification of functionalized silica gels, and chromatograms of various analytes in the modified stationary phase are shown in Figure 12. The diverse analytes separated in this study indicated that the retention mechanisms were influenced by hydrophobic, π - π stacking, and electrostatic interactions (Yang *et al.*, 2022).

Antimicrobial performance

The antimicrobial properties of HCDs are believed to relate the production of reactive oxygen species (ROS), the disruption of bacterial membranes, and the degradation of biofilm structures. One approach to trigger the antibacterial effectiveness of HCDs is through the generation of ROS using low-power blue light (470 nm). In this process, HCDs act as both photosensitizers and photocatalysts, triggering the production of ROS and

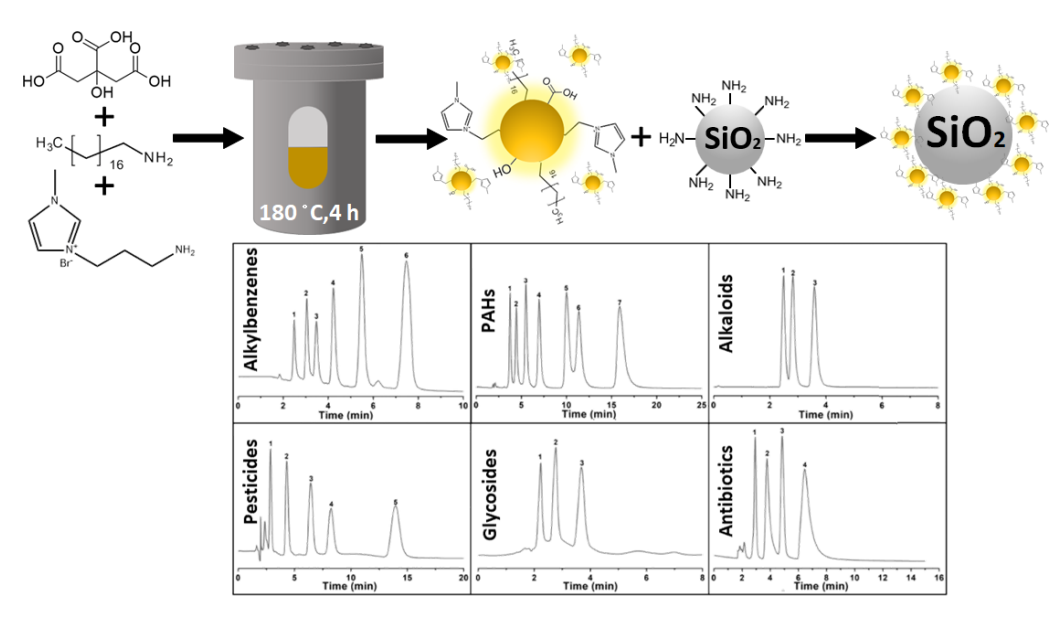


Figure 12. A hypothetical diagram of the synthesis of HCDs and modification of stationary phases, and chromatograms of alkylbenzenes, PAHs, alkaloids, pesticides, glycosides, and antibiotics on the modified column (adapted from Yang et al., 2022).

hydroxyl radicals (Bodik *et al.*, 2018; Budimir *et al.*, 2021; Kováčová *et al.*, 2020). These reactive species disrupt redox balance, which interferes with bacterial metabolism and affects cell membranes, mitochondria, proteins, and DNA. This ultimately results in the death of microorganisms (Chu *et al.*, 2022). As stated earlier, HCDs can produce ROS when exposed to blue light and are capable of withstanding photobleaching (Budimir *et al.*, 2021). Moreover, when subjected to radiation at a specific wavelength, HCDs generate electron-hole pairs (e-/h+) that promote electron transfer and the subsequent production of ROS such as hydroxyl radicals (•OH) and superoxide ions (O2^{•-}), which effectively deactivate microorganisms (Zhang *et al.*, 2018).

Carbon dots exhibit varying levels of antimicrobial activity against different microorganisms. Gram-negative bacteria possess a delicate peptidoglycan layer situated between two membranes, which are composed of lipopolysaccharides and phospholipids. Hydrophilic antibacterial compounds exhibit limited efficacy against Gram-negative bacteria because these antimicrobials cannot effectively cross the hydrophobic layers of cell membranes (Ezati et al., 2022). In contrast, hydrophobic antimicrobial compounds can easily penetrate cell membranes (Bandi et al., 2020; Mousavi Khaneghah et al., 2018) and disrupt their integrity, leading to the leakage of cytosol from the cell, ultimately causing cell death (Figure 13; Jian et al., 2020).

Hydrophobic carbon dots can interact with microbial biofilms on different surfaces by affecting microbial adhesion, biofilm matrix stability, and microbial behavior within the biofilm structure. In this case, HCDs can be directly added to biofilm-contaminated surfaces or incorporated into a thin-layer film. In a particular study, scientists applied consistent and uniform thin films incorporating HCDs onto various substrates, such as SiO₂/Si, glass, and mica, and investigated the biofilm formation of several bacterial strains (Stanković et al., 2018). The results showed that bacterial strains had an affinity for hydrophobic surfaces, increasing their likelihood of attachment. However, following blue light exposure, the metabolic activity, which corresponds to the number of Bacilluscereus and Pseudomonas aeruginosa, decreased by approximately 50% and 78%, respectively. Additionally, the results demonstrated that the majority of Escherichia coli strains were eradicated within 1 h.

Budimir *et al.* (2021) introduced a photoactive HCD-based composite film in which Pluronic 68-derived HCDs were integrated into a PU polymer matrix. The films were prepared using the *ex-situ* method by submerging PU stripes in a solution containing HCDs dispersed in toluene, followed by drying in the vacuum furnace overnight at 80°C. Also, Marković *et al.* (2022) fabricated the antibacterial composite consisting of HCD riboflavin-based CDs and commercial PU films by submerging PU films in riboflavin-derived CDs dispersed in acetone, followed by drying in a vacuum furnace at 80°C. These approaches produce hydrophobic polymer surfaces with decreased microbial adhesion, which is ideal for medical devices, self-cleaning textiles, and food packaging applications (Bodik *et al.*, 2018; Marković *et al.*, 2019).

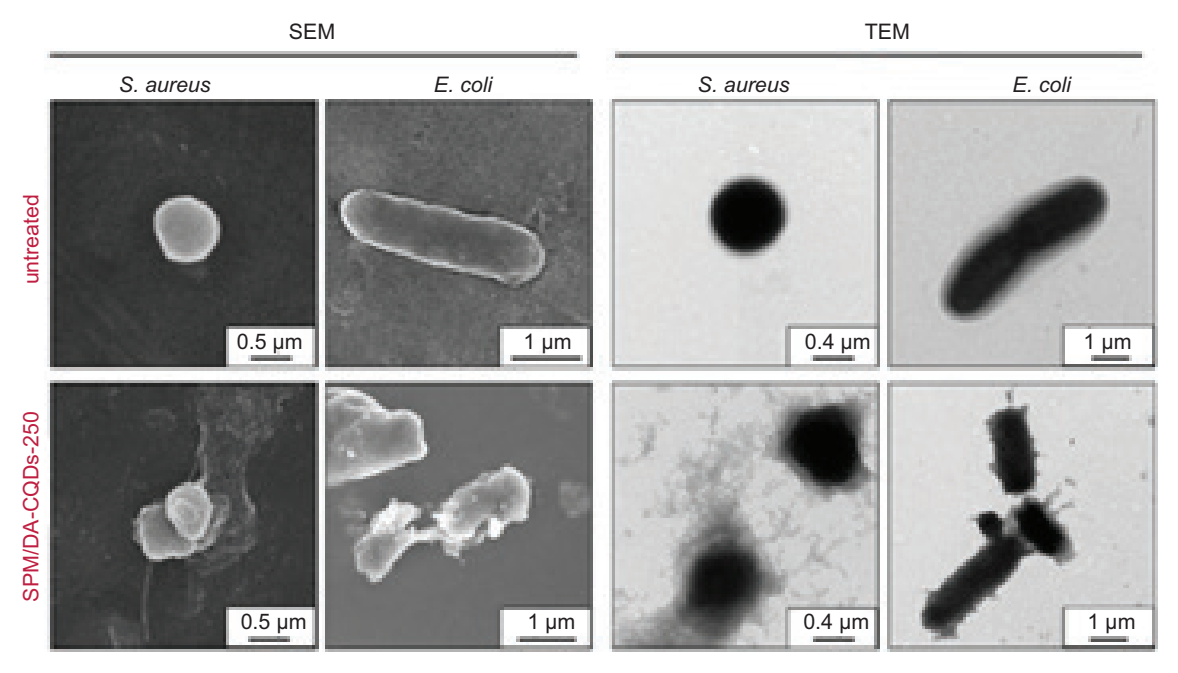


Figure 13. Scanning electron microscopy (SEM) and transmission electron microscopy (TEM) of untreated *S. aureus* and *E. coli* cells following treatment with CDs derived from spermine and dopamine (adapted from Jian *et al.*, 2020).

Enhancing textiles with HCDs ensures cleanliness of hospital garments and eliminates the need for disinfection. Kováčová et al. (2020) selected two types of transparent polyether-urethane and polyester-urethane polymers as substrates for the embedding of HCDs through dip coating. These composites can be coated onto different types of textiles (using lamination procedure). Their findings revealed a significant reduction in the Staphylococcus spp. population. The antimicrobial effect of modified surfaces relies on the generation of ROS, which induce oxidative stress and subsequent damage to bacteria (Kováčová et al., 2020; Marković et al., 2019). Marković et al. (2019) developed an antibacterial surface by incorporating HCDs into a PDMS polymer matrix to create a nanocomposite. When exposed to blue light (470 nm, for 15 min), the nanocomposite generated singlet oxygen, leading to eradication of Klebsiella pneumoniae, E. coli, and S. aureus. A swelling-shrinkage-encapsulation approach was utilized to encapsulate HCDs in polymer. The nanocomposites based on HCDs were found to generate singlet oxygen upon exposure to blue light at 470 nm, effectively targeting and eliminating Gram-negative bacteria, such as K. pneumonia and E. coli as well as Gram-positive bacteria, such as Listeria monocytogenes and S. aureus (Ghosal et al., 2021). The HCDs derived from riboflavin embedded in innovative PU composite films exhibit high potential to generate ROS, photocatalytic activity, low dark cytotoxicity (against MRC-5 cells), and robust antibacterial activity, especially against *E. coli*. Significantly, the extended lifetime of singlet oxygen production, along with favorable kinetics for generating singlet oxygen and superoxide anions, encouraged the use of the developed nanocomposites as antimicrobial surfaces in healthcare environments where numerous highcontact items are present (Marković et al., 2022). The photocatalytic activity of HCDs embedded in transparent PU demonstrated degradation of Rose Bengal dye up to 86% of the dye solution within 3 h of exposure to blue light (Kováčová *et al.*, 2018). They attributed this behavior to the substantial production of ROS during irradiation.

Recently, Razavi *et al.* (2024) described an easy method for synthesizing Janus nanoparticles that combine beeswax-based HCDs with hydrophilic carboxymethyl cellulose. They utilized a hydrothermal technique, placing a mixture of beeswax dispersed in acetic acid and heating at 200°C for 10 h. The antibacterial evaluation of the HCDs revealed a minimum inhibitory concentration of 0.02 mg/mL against *E. coli* and 0.04 mg/mL against *L. monocytogenes*. Additionally, the HCDs displayed significant antioxidant properties. Furthermore, the synthesized HCDs were incorporated into minced beef, serving as innovative preservatives that effectively reduced both chemical and microbial spoilage during storage.

Development of fluorescent inks, light-emitting diode, and fingerprint detection

Owing to their impressive optical features and ability to dissolve in various solvents, long-wavelength-emitting HCDs hold great promise for applications in optoelectronics as well as innovative solid-state lighting and monitoring technology (Chen *et al.*, 2018; Khan *et al.*, 2018; Zhao *et al.*, 2020). Xu *et al.* (2023) synthesized solid luminescent HCDs from dithiosalicylic acid and acetic acid precursors. The emission behavior of HCDs, including red, yellow, and green AIE, can be tuned by incorporating melamine, urea, and sulfonamide in the formulation during synthesis (Figure 14).

Fluorescent materials significantly increase contrast and sensitivity compared to standard white and black powders. Xu *et al.* (2023) effectively demonstrated the

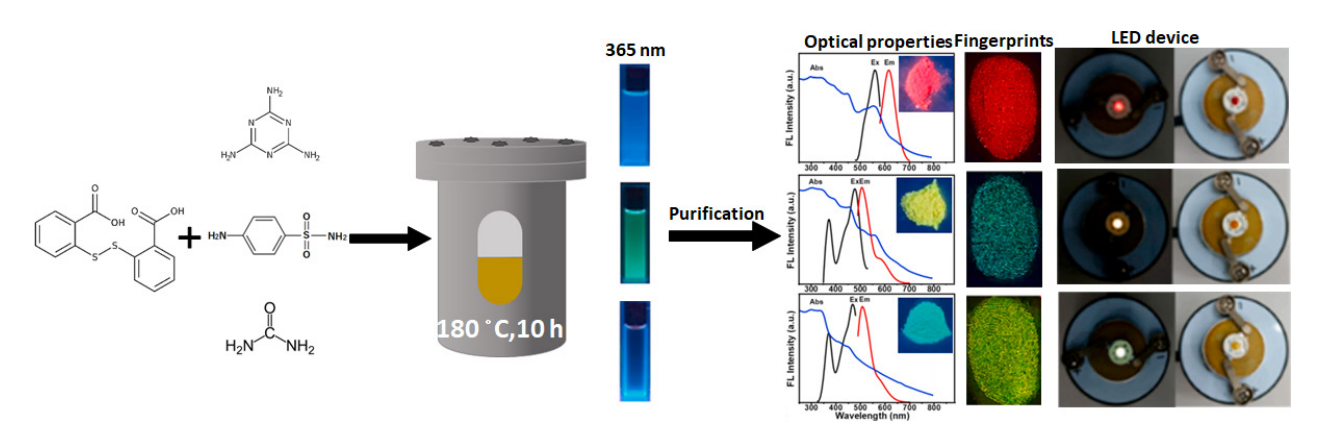


Figure 14 Synthesis process, photographs of three HCDs under 365-nm UV light, optical characteristics (FL excitation, emission spectra, and UV-vis spectra), photograph of powder-stained latent fingerprints on glass substrates under UV light irradiation, and photos of fabricated LED devices before and after power connected (adapted from Xu et al., 2023).

visualization of latent fingerprints on a glass surface by using the photoluminescent properties of lipid-soluble HCDs (Figure 14). The pronounced contrast of fluorescent signals from various features in the latent fingerprint, including bifurcations, islands, terminations, eyes, nuclei, ridge divergence, and intersection points, enables the differentiation of various sample patterns.

In the case of many water-soluble CDs, fluorescence quenching happens either when aggregates form or in a solvent-free environment. However, if the cores of CDs are adequately spaced apart, fluorescence quenching can be prevented. In HCDs, the photoluminescent centers are distanced from one another by alkyl chains, which inhibit fluorescence quenching and make them particularly appealing for applications in fluorescent inks (Yin et al., 2019). Yin et al. (2019) used a mixture of ethanol and glycerol with a volume ratio of 1:1, and the optimum concentration of HCDs synthesized through refluxing of dodecylamine (C₁₂–NH₂) in chlorobenzene as fluorescence ink. Figure 15A shows letters written on a silica gel plate with bright emission under 365-nm UV radiation.

Yang et al. (2019) developed HCDs using melamine, dithiosalicylic acid, and acetic acid to formulate a luminescence ink capable of reversible two-switch mode functionality. The resulting N- and S-doped HCDs exhibited varying luminescent properties based on the conditions of treatment and irradiation. When exposed to 365-nm UV light, the printed filter paper produced a blue emission, while no luminescence was detected under 254-nm UV light. When printing was performed with an aqueous suspension of HCDs, followed by air-drying, pink and red emissions were observed when irradiated with UV at 365 nm and 254 nm, respectively. Furthermore, after re-dissolution in ethanol and drying, a change from pink to blue emission (at 365-nm UV) and the quenching of red fluorescence (at 254 nm) was observed (Figure 15B).

Other applications

In photovoltaic applications, one of the drawbacks of CDs is the existence of a large number of surface defects,

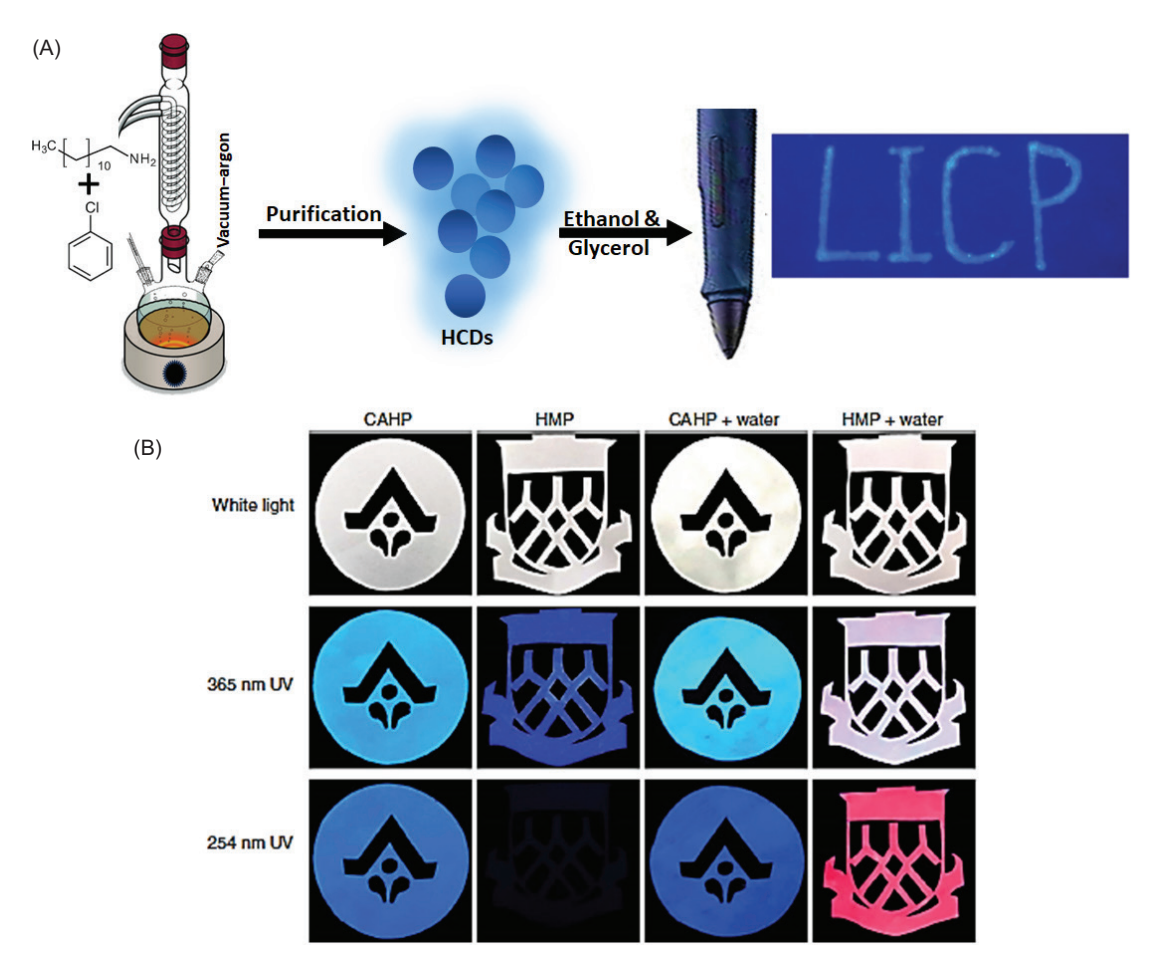


Figure 15. An image of letters written with HCD ink on a silica plate, captured under UV light (365 nm) (A) (with permission from in Yin et al., 2019). (B) A mark pen filled with HCD solution (HMP) used as an anti-counterfeiting tool, shown alongside a standard commercially available highlighter pen (CAHP) (adapted from Yang et al., 2019).

which impair the efficiency of charge transfer. To address this issue, Coşkun *et al.* (2022) synthesized a water-insoluble CD using a calix[4]pyrrole precursor that displayed excitation-dependent emission properties. The produced HCDs exhibited a quantum yield (QY) exceeding 60%, with particle sizes ranging from roughly 4–10 nm, a graphitic framework, and minimal surface imperfections. These characteristics make them a promising option for use as an additive in solar cell applications. The researchers introduced CDs as additives to the photoactive layer (poly(3-hexylthiophene-2,5-diyl):(6,6)-phenyl C61 butyric acid methyl ester blend) and reported enhanced synergistic effects of photovoltaic parameters, charge generation, ohmic contact, and extraction efficiency more than the traditional ones.

Hydrophobic carbon dots are also used in the development of nanocomposites designed to adsorb and eliminate radioactive pollutants, such as iodine (molecular I₂), from aqueous waste solutions. Zheng et al. (2019) synthesized HCDs from CPC and NaOH through a chemical oxidation route. The carbonization process resulted in a wine-red-colored solution, from which the HCDs were extracted using petroleum ether. The HCDs were modified with natural cotton fibers through simple physical adsorption via dip coating. The constructed nano-adsorbent had an excellent stability in water and its efficiency in absorbing I₂ in an aqueous solution, with an improved adsorption capacity of approximately 6.8 times higher than that of the unmodified cotton fiber. Additionally, the adsorbed I_2 can be easily released by immersing it in a different aqueous solution (pH 1) containing an excess amount of Na₂SO₂.

The development of high-quality membranes with effective separation capabilities is crucial for forward osmosis (FO) technology. Zhang et al. (2021) introduced a thin-film composite membrane incorporating HCDs to optimize water channels for FO applications. These HCDs acted as nanofillers within a polyacrylonitrile (PAN) support layer. The analysis of the PAN membrane with HCDs revealed a uniform pore distribution with a reduced average pore size, while the membrane's surface exhibited consistent finger-like hierarchical channels and micro-convex structures along the pore walls. The HCDenhanced membrane achieved a high water flux of 15.47 L m⁻² h⁻¹ and a low reverse salt flux of 2.9 g m⁻² h⁻¹ using a 1 mol/L NaCl draw solution. These findings suggest that HCDs can serve as effective water flux modifiers to enhance FO performance.

Carbon dots attached to fluorescent labels are used for tumor diagnosis to provide information about malignancy, progression, and location (Boakye-Yiadom *et al.*, 2019). In addition, the longer-wavelength fluorescence emission of HCDs is preferred for better differentiation

from the background of live tissues, and minimizes radiation damage, compared to shorter-wavelength excitation. Compared to hydrophilic CDs, HCDs exhibit significantly enhanced cell imaging capabilities because of their increased traverse across cell membranes and accumulation within the cells (Paul *et al.*, 2022). For example, Mao *et al.* (2015) synthesized hydrophilic CDs and HCDs using a single-pot hydrothermal process involving the use of 1-butyl-3-methylimidazolium hexafluorophosphate as a carbon source in an $\rm H_3PO_4$ —ethanol medium. Fluorescent CDs were used to label live HeLa cells, and the labeled cells were examined with an inverted fluorescence microscope.

Carbon dots are used to deliver drugs to specific cells and tissues. Owing to their small size, CDs can readily cross biological barriers (Zhang *et al.*, 2021; Zhou *et al.*, 2019). For example, Shu *et al.* (2017) produced hydrophilic and organophilic CDs through a hydrothermal method using 1,3-dibutylimidazolium nitrate in the presence of sulfuric acid. HCDs showed excellent compatibility with biological systems, bright PL, low levels of toxicity, effective drug-loading capacity, and swift infiltration into HeLa cells.

Photodynamic therapy (PDT) and photothermal therapy rely on clinical conditions as well as the quality of external light sources and the effectiveness of light-activating photosensitizers. Photothermal therapy relies on heat generation by photosensitizers to eliminate cancer cells, while photodynamic therapy works by producing ROS. Wen et al. (2019) recently used NIR-light-emitting HCDs derived from pheophytin for PDT. In their work, Wen et al. (2019) investigated photodynamic behavior, including singlet oxygen formation and ROS generation upon NIR irradiation (671-nm laser), cellular uptake behavior, cytotoxicity (on 4T1 cells), and photostability of HCDs. The researchers reported that the HCDs exhibited excellent photostability, as observed through their consistent absorption spectra under different laser irradiation periods. The treated cells initially showed high viability; however, upon exposure to laser irradiation, their viability declined due to the generation of singlet oxygen, as indicated by green fluorescence. In vivo imaging of mice with tumors revealed that HCDs gradually accumulated at the tumor site following intravenous administration, with a higher concentration at the tumor, compared to other tissues and organs. An in vivo study validated the effectiveness of HCDs in PDT against 4TI tumors in mice.

Conclusions and Future Trends

Owing to their sensitivity to light, compatibility with lipids, availability of raw materials, and low toxicity profile,

HCDs have emerged as a significant focus in nanoscience and food science. Despite their promising attributes, the full potential of HCDs remains largely unexplored. This review highlights the immense promise of HCDs in a multitude of fields, such as chemosensors, antimicrobials, and food safety applications. One of the most notable features of HCDs is their optical properties, particularly strong and tunable fluorescence. The PL of HCDs is adjusted by modifying their size, surface functional groups, and the types of precursors used in their synthesis. Additionally, HCDs with unique luminescence properties (ability to emit light in different colors) are ideal for use in light-emitting diodes, solar cells, photodetectors, and optoelectronic devices. The integration of HCDs into these devices could lead to improvement in performance, energy efficiency, and device longevity for the manufacturing of food-related materials and instruments.

Since the emission of HCDs can be fine-tuned by adjusting condensation reactions, performing chemical modifications, or introducing heteroatoms, it is possible to create chemosensors and biosensors for a wide range of substances, including heavy metal ions, toxins, and specific compounds, suitable for both laboratory applications and commercial kits. One of the most promising uses of HCDs is their antimicrobial properties. Their photocatalytic, photothermal, and photoluminescent characteristics enable them to effectively inhibit microbial growth and prevent biofouling. Additionally, modifying the surface of HCDs can enhance their interactions with microbial cells, thereby boosting their antimicrobial effectiveness. The photoluminescent characteristics of HCDs can also be utilized in smart packaging solutions, which signal the freshness or spoilage of food items through color changes. This advancement can offer consumers immediate insights into food quality, help minimize food waste, and enhance overall food safety.

Despite the potential applications of HCDs, several obstacles are to overcome to fully harness their capabilities. The lack of environmentally sustainable synthesis methods, complex multi-step functionalization procedures, production of HCDs with a wide size distribution, and the necessity for additional purification steps that can be both time-consuming and labor-intensive are significant challenges in this area. Furthermore, securing approval from health and environmental regulatory bodies is essential to ensure that HCDs are safe and comply with regulations for various uses. Extensive toxicity assessments and environmental impact evaluations are needed to verify the safety of HCDs for both human health and the environment. In summary, while there are inherent difficulties in utilizing HCDs, ongoing

research initiatives offer promise for overcoming these challenges.

Data Availability Statement

Data are made available upon request.

Author Contributions

Conceptualization: Rahim Molaei, Roghayieh Razavi, Mehran Moradi; writing of original draft: Rahim Molaei, Roghayieh Razavi, Abdullah Khalid Omer, Anita Lotfi Javid, Negar Nikfarjam; review and editing of paper: Rahim Molaei, Roghayieh Razavi, Parya Ezati, Loong-Tak Lim, Mehran Moradi.

Conflicts of Interest

The authors declared no conflict of interest.

Funding

This work is based upon research funded by Iran National Science Foundation (INSF) under project No. 4013305. The authors did not receive any finical support for publication.

References

Ali, H., Bhunia, S.K., Dalal, C. and Jana, N.R., 2016. Red fluorescent carbon nanoparticle-based cell imaging probe. ACS Applied Materials & Interfaces 8: 9305–9313. https://doi.org/10.1021/ acsami.5b11318

Amézqueta, S., Subirats, X., Fuguet, E., Rosés, M. and Ràfols, C., 2020. Octanol-water partition constant. In: Poole, C.F (eds.). Liquid-phase extraction. Elsevier, Amsterdam, the Netherlands, pp. 183–208. https://doi.org/10.1016/B978-0-12-816911-7.00006-2

Arshad, F. and Sk, M.P., 2019. Aggregation-induced red shift in N,S-doped chiral carbon dot emissions for moisture sensing. New Journal of Chemistry 43: 13240–13248. https://doi.org/10.1039/C9NI03009C

Bandi, R., Kannikanti, H. Gavash, Dadigala, R., Gangapuram, B. Reddy, Rao Vaidya, J., Guttena, V., 2020. One step synthesis of hydrophobic carbon dots powder with solid state emission and application in rapid visualization of latent fingerprints. Optical Materials (Amsterdam). 109: 110349. https://doi.org/10.1016/j.optmat.2020.110349

Barnoud, J., Rossi, G., Marrink, S.J. and Monticelli, L., 2014. Hydrophobic compounds reshape membrane domains. PLoS Computational Biology 10: e1003873.

- Bartolomei, B., Dosso, J. and Prato, M., 2021. New trends in nonconventional carbon dot synthesis. Trends in Chemistry 3: 943– 953. https://doi.org/10.1016/j.trechm.2021.09.003
- Bhunia, S.K., Saha, A., Maity, A.R., Ray, S.C. and Jana, N.R., 2013.

 Carbon nanoparticle-based fluorescent bioimaging probes.

 Scientific Reports 3: 1–7. https://doi.org/10.1038/srep01473
- Boakye-Yiadom, K.O., Kesse, S., Opoku-Damoah, Y., Filli, M.S., Aquib, M., Joelle, M.M.B., Farooq, M.A., Mavlyanova, R., Raza, F., Bavi, R. and Wang, B., 2019. Carbon dots: applications in bioimaging and theranostics. International Journal of Pharmaceutics 564: 308–317. https://doi.org/10.1016/j. ijpharm.2019.04.055
- Bodik, M., Siffalovic, P., Nadazdy, P., Benkovicova, M., Markovic, Z., Chlpik, J., Cirak, J., Kotlar, M., Micusik, M. and Jergel, M., 2018. On the formation of hydrophobic carbon quantum dots Langmuir films and their transfer onto solid substrates. Diamond and Related Materials 83: 170–176. https://doi. org/10.1016/j.diamond.2018.02.011
- Bourlinos, A.B., Karakassides, M.A., Kouloumpis, A., Gournis, D., Bakandritsos, A., Papagiannouli, I., Aloukos, P., Couris, S., Hola, K., Zboril, R., Krysmann, M. and Giannelis, E.P., 2013. Synthesis, characterization and nonlinear optical response of organophilic carbon dots. Carbon (N.Y.) 61: 640–643. https:// doi.org/10.1016/j.carbon.2013.05.017
- Bourlinos, A.B., Stassinopoulos, A., Anglos, D., Zboril, R., Karakassides, M. and Giannelis, E.P., 2008. Surface functionalized carbogenic quantum dots. Small 4: 455–458. https://doi. org/10.1002/smll.200700578
- Budimir, M., Marković, Z., Vajdak, J., Jovanović, S., Kubat, P., Humpoliček, P., Mičušik, M., Danko, M., Barras, A., Milivojević, D., Špitalsky, Z., Boukherroub, R. and Marković, B.T., 2021. Enhanced visible light-triggered antibacterial activity of carbon quantum dots/polyurethane nanocomposites by gamma rays induced pre-treatment. Radiation Physics and Chemistry 185: 109499. https://doi.org/10.1016/j.radphyschem.2021.109499
- Çalhan, S.D., Alaş, M.Ö., Aşık, M., Kaya, F.N.D. and Genç, R., 2018.

 One-pot synthesis of hydrophilic and hydrophobic fluorescent carbon dots using deep eutectic solvents as designer reaction media. Journal of Materials Science 53: 15362–15375. https://doi.org/10.1007/s10853-018-2723-4
- Chatterjee, A., Ruturaj, Chakraborty, M.P., Nandi, S. and Purkayastha, P., 2022. Biocompatible and optically stable hydrophobic fluorescent carbon dots for isolation and imaging of lipid rafts in model membrane. Analytical and Bioanalytical Chemistry 414: 6055–6067. https://doi.org/10.1007/s00216-022-04165-6
- Chen, J., Gong, Z., Tang, W., Row, K.H. and Qiu, H., 2021a. Carbon dots in sample preparation and chromatographic separation: recent advances and future prospects. Trends in Analytical Chemistry (TrAC) 134: 116135. https://doi.org/10.1016/j. trac.2020.116135
- Chen, J., Yuan, N., Jiang, D., Lei, Q., Liu, B., Tang, W., Row, K.H. and Qiu, H., 2021b. Octadecylamine and glucose-coderived hydrophobic carbon dots-modified porous silica for chromatographic separation. Chinese Chemical Letters 32: 3398–3401. https:// doi.org/10.1016/j.cclet.2021.04.052

- Chen, T., Zhang, Q., Xie, Z., Tan, C., Chen, P., Zeng, Y., Wang, F., Liu, H., Liu, Y., Liu, G. and Lv, W., 2018. Carbon nitride modified hexagonal boron nitride interface as highly efficient blue LED light-driven photocatalyst. Applied Catalysis B: Environment and Energy 238: 410–421. https://doi.org/10.1016/j. apcatb.2018.07.053
- Chen, X., Zhang, Z. and Zhao, J., 2015. Purification, organophilicity and transparent fluorescent bulk material fabrication derived from hydrophilic carbon dots. RSC Advances 5: 14492–14496. https://doi.org/10.1039/c4ra15684f
- Cheng, F., An, X., Zheng, C. and Cao, S., 2015. Green synthesis of fluorescent hydrophobic carbon quantum dots and their use for 2, 4, 6-trinitrophenol detection. RSC Advances 5: 93360–93363. https://doi.org/10.1039/C5RA19029K
- Chisari, M., Eisenman, L.N., Krishnan, K., Bandyopadhyaya, A.K., Wang, C., Taylor, A., Benz, A., Covey, D.F., Zorumski, C.F. and Mennerick, S., 2009. The influence of neuroactive steroid lipophilicity on GABAA receptor modulation: evidence for a lowaffinity interaction. Journal of Neurophysiology 102: 1254–1264.
- Choi, C.A., Mazrad, Z.A.I., Ryu, J.H., In, I., Lee, K.D. and Park, S.Y., 2018. Membrane and nucleus targeting for highly sensitive cancer cell detection using pyrophosphate and alkaline phosphatase activity-mediated fluorescence switching of functionalized carbon dots. Journal of Materials Chemistry B 6: 5992–6001.
- Chu, K.-W., Lee, S.L., Chang, C.-J. and Liu, L., 2019. Recent progress of carbon dot precursors and photocatalysis applications. Polymers (Basel) 11, 689. https://doi.org/10.3390/ polym11040689
- Chu, X., Wang, M., Shi, S., Sun, B., Song, Q., Xu, W., Shen, J. and Zhou, N., 2022. A review on properties and antibacterial applications of polymer-functionalized carbon dots. Journal of Materials Science 57: 12752–12781. https://doi.org/10.1007/ s10853-022-07394-3
- Cook, E., Labiento, G. and Chauhan, B.P.S., 2021. Fundamental methods for the phase transfer of nanoparticles. Molecules 26(20): 6170. https://doi.org/10.3390/molecules26206170
- Coşkun, Y., Ünlü, F.Y., Yılmaz, T., Türker, Y., Aydogan, A., Kuş, M. and Ünlü, C., 2022. Development of highly luminescent water-insoluble carbon dots by using Calix[4]pyrrole as the carbon precursor and their potential application in organic solar cells. ACS Omega 7: 18840–18851. https://doi.org/10.1021/acsomega.2c01795
- Das, R., Bandyopadhyay, R. and Pramanik, P., 2018. Carbon quantum dots from natural resource: a review. Materials Today Chemistry 8: 96–109. https://doi.org/10.1016/j.mtchem.2018.03.003
- De, S.K., Maity, A., Bagchi, D. and Chakraborty, A., 2021. Lipid phase dependent distinct emission behaviour of hydrophobic carbon dots: C-dot based membrane probes. Chemical Communications 57: 9080–9083. https://doi.org/10.1039/D1CC01941D
- de Andrés, F. and Ríos, Á., 2021. Carbon dots separative techniques: tools-objective towards green analytical nanometrology focused on bioanalysis. Microchemical Journal 161: 105773. https://doi.org/10.1016/j.microc.2020.105773
- Dutta, G.K. and Karak, N., 2022. Overview of carbon dot synthesis. In: Khan, R., Murali, s., Gogoi, S (eds.). Carbon dots in

- agricultural systems. Elsevier, Amsterdam, the Netherlands, pp. 39-68. https://doi.org/10.1016/B978-0-323-90260-1.00010-3
- Ezati, P., Rhim, J.-W., Molaei, R., Priyadarshi, R., Roy, S., Min, S., Kim, Y.H., Lee, S.-G. and Han, S., 2022. Preparation and characterization of B, S, and N-doped glucose carbon dots: antibacterial, antifungal, and antioxidant activity. Sustainable Materials and Technologies 32: e00397. https://doi.org/10.1016/j.susmat.2022.e00397
- Fahmi, M.Z., Wibowo, D.L.N., Sakti, S.C.W. and Lee, H.V., 2020. Human serum albumin capsulated hydrophobic carbon nanodots as staining agent on HeLa tumor cell. Materials Chemistry and Physics 239: 122266. https://doi.org/10.1016/j.matchemphys. 2019.122266
- Fan, Y., Yang, X., Yin, C., Ma, C. and Zhou, X., 2019. Blue- and green-emitting hydrophobic carbon dots: preparation, optical transition, and carbon dot-loading. Nanotechnology 30: 265704. https://doi.org/10.1088/1361-6528/ab0b14
- Feng, J., Chen, S., Yu, Y. and Wang, J., 2020. Red-emission hydrophobic porphyrin structure carbon dots linked with transferrin for cell imaging. Talanta 217: 121014. https://doi.org/10.1016/j. talanta.2020.121014
- Fu, G., Chen, J. and Qiu, H., 2022a. Deep eutectic solvents-derivated carbon dots-decorated silica stationary phase with enhanced separation selectivity in reversed-phase liquid chromatography. Journal of Chromatography A 1681: 463425. https://doi. org/10.1016/j.chroma.2022.463425
- Fu, G., Gao, C., Quan, K., Li, H., Qiu, H. and Chen, J., 2022b. Phosphorus-doped deep eutectic solvent-derived carbon dots-modified silica as a mixed-mode stationary phase for reversed-phase and hydrophilic interaction chromatography. Analytical and Bioanalytical Chemistry 6: 1342. https://doi. org/10.1007/s00216-022-04405-9
- Galyean, A.A., Behr, M.R. and Cash, K.J., 2018. Ionophore-based optical nanosensors incorporating hydrophobic carbon dots and a pH-sensitive quencher dye for sodium detection. Analyst 143: 458–465. https://doi.org/10.1039/C7AN01382E
- Ganiga, M., Mani, N.P. and Cyriac, J., 2018. Synthesis of organophilic carbon dots, selective screening of trinitrophenol and a comprehensive understanding of luminescence quenching mechanism. Chemistry Select 3: 4663–4668. https://doi.org/10.1002/slct.201702646
- Gao, W., Zhou, Y., Xu, C., Guo, M., Qi, Z., Peng, X. and Gao, B., 2019. Bright hydrophilic and organophilic fluorescence carbon dots: one-pot fabrication and multi-functional applications at visualized Au3+ detection in cell and white light-emitting devices. Sensors & Actuators, B: Chemical 281: 905–911. https://doi.org/10.1016/j.snb.2018.11.024
- Garg, A.K., Dalal, C., Kaushik, J., Anand, S.R. and Sonkar, S.K., 2022.
 Selective sensing of explosive nitrophenol compounds by using hydrophobic carbon nanoparticles. Materials Today Sustainability 20: 100202. https://doi.org/10.1016/j.mtsust.2022.100202
- Ghosal, K., Kováčová, M., Humpolíček, P., Vajďák, J., Bodík, M. and Špitalský, Z., 2021. Antibacterial photodynamic activity of hydrophobic carbon quantum dots and polycaprolactone based nanocomposite processed via both electrospinning and solvent

- casting method. Photodiagnosis and Photodynamic Therapy 35: 102455. https://doi.org/10.1016/j.pdpdt.2021.102455
- González-González, R.B., González, L.T., Madou, M., Leyva-Porras, C., Martinez-Chapa, S.O. and Mendoza, A., 2022. Synthesis, purification, and characterization of carbon dots from nonactivated and activated pyrolytic carbon black. Nanomaterials 12: 298. https://doi.org/10.3390/nano12030298
- Gude, V., 2014. Synthesis of hydrophobic photoluminescent carbon nanodots by using L-tyrosine and citric acid through a thermal oxidation route. Beilstein Journal of Nanotechnology 5: 1513–1522.
- Guha, A. and Ghosh, D., 2022. A toxicologic review of quantum dots: recent insights and future directions. In: Barik, P. and Mondal, S. (eds.). Application of quantum dots in biology and medicine: recent advances Springer Nature, Singapore, pp. 67–90. https://doi.org/10.1007/978-981-19-3144-4_4
- Guo, T., Wang, X., Hong, X., Xu, W., Shu, Y. and Wang, J., 2022. Modulation of the binding ability to biomacromolecule, cyto-toxicity and cellular imaging property for ionic liquid mediated carbon dots. Colloids Surfaces B Biointerfaces 216: 112552. https://doi.org/10.1016/j.colsurfb.2022.112552
- Guo, T., Wang, X., Zhao, C., Shu, Y. and Wang, J., 2021. Precise regulation of the properties of hydrophobic carbon dots by manipulating the structural features of precursor ionic liquids. Biomaterials Science 9: 3127–3135. https://doi.org/10.1039/ D1BM00090I
- Han, S., Zhang, H., Zhang, J., Xie, Y., Liu, L., Wang, H., Li, X., Liu, W. and Tang, Y., 2014. Fabrication, gradient extraction and surface polarity-dependent photoluminescence of cow milkderived carbon dots. RSC Advances 4: 58084–58089. https://doi. org/10.1039/C4RA09520K
- Hardman, R., 2006. A toxicologic review of quantum dots: toxicity depends on physicochemical and environmental factors. Environmental Health Perspectives 114(2): 165–172. https://doi.org/10.1289/ehp.8284
- He, M., Jiang, X., Wang, X., Xiang, G. and He, L., 2024. Solvent-free synthesis of recyclable hydrophobic carbon dots for highly selective detecting curcumin in food samples. Microchemical Journal 199: 109898. https://doi.org/10.1016/j.microc.2024.109898
- Jana, D., Wang, D., Rajendran, P., Bindra, A.K., Guo, Y., Liu, J., Pramanik, M. and Zhao, Y., 2021. Hybrid carbon dot assembly as a reactive oxygen species nanogenerator for ultrasound-assisted tumor ablation. Journal of the American Chemical Society 1: 2328–2338. https://doi.org/10.1021/jacsau.1c00422
- Jian, H.-J., Yu, J., Li, Y.-J., Unnikrishnan, B., Huang, Y.-F., Luo, L.-J., Hui-Kang Ma, D., Harroun, S.G., Chang, H.-T., Lin, H.-J., Lai, J.-Y. and Huang, C.-C., 2020. Highly adhesive carbon quantum dots from biogenic amines for prevention of biofilm formation. Chemical Engineering Journal 386: 123913. https://doi. org/10.1016/j.cej.2019.123913
- Jiang, D., Chen, J., Guan, M. and Qiu, H., 2021. Octadecylimidazolium ionic liquids-functionalized carbon dots and their precursor co-immobilized silica as hydrophobic chromatographic stationary phase with enhanced shape selectivity. Talanta 233: 122513. https://doi.org/10.1016/j.talanta.2021.122513

- Khairol Anuar, N.K., Tan, H.L., Lim, Y.P., So'aib, M.S. and Abu Bakar, N.F., 2021. A review on multifunctional carbon-dots synthesized from biomass waste: design/ fabrication, characterization and applications. Frontiers in Energy Research 9: 67. https://doi.org/10.3389/fenrg.2021.626549
- Khan, W.U., Wang, D. and Wang, Y., 2018. Highly green emissive nitrogen-doped carbon dots with excellent thermal stability for bioimaging and solid-state LED. Inorganic Chemistry 57(24): 15229–15239. https://doi.org/10.1021/acs.inorgchem.8b02524
- Kong, D., Yan, F., Luo, Y., Ye, Q., Zhou, S. and Chen, L., 2017. Amphiphilic carbon dots for sensitive detection, intracellular imaging of Al³⁺. Analytica Chimica Acta 953: 63–70. https://doi. org/10.1016/j.aca.2016.11.049
- Koutsioukis, A., Akouros, A., Zboril, R., Georgakilas, V., 2018. Solid phase extraction for the purification of violet, blue, green and yellow emitting carbon dots. Nanoscale 10: 11293–11296. https://doi.org/10.1039/C8NR03668C
- Kováčová, M., Kleinová, A., Vajďák, J., Humpolíček, P., Kubát, P., Bodík, M., Marković, Z. and Špitálský, Z., 2020. Photodynamicactive smart biocompatible material for an antibacterial surface coating. Journal of Photochemistry and Photobiology B: Biology 211: 112012. https://doi.org/10.1016/j.jphotobiol.2020.112012
- Kováčová, M., Marković, Z.M., Humpolicek, P., Micusik, M., Svajdlenkova, H., Kleinova, A., Danko, M., Kubat, P., Vajdak, J. and Capakova, Z., 2018. Carbon quantum dots modified polyurethane nanocomposite as effective photocatalytic and antibacterial agents. ACS Biomaterials Science & Engineering 4: 3983–3993. https://doi.org/10.1021/acsbiomaterials.8b00582
- Kumar, R., Kumar, V.B. and Gedanken, A., 2020. Sonochemical synthesis of carbon dots, mechanism, effect of parameters, and catalytic, energy, biomedical and tissue engineering applications. Ultrason. Sonochem 64: 105009. https://doi.org/10.1016/j.ultsonch.2020.105009
- Li, S., Li, L., Tu, H., Zhang, H., Silvester, D.S., C, C.E.B., Hou, H., Zou, G. and Ji, X., 2021a. The development of carbon dots: from the perspective of materials chemistry. Materials Today 51: 188–207. https://doi.org/10.1016/j.mattod.2021.07.028
- Li, T., Li, Z., Huang, T. and Tian, L., 2021b. Carbon quantum dotbased sensors for food safety. Sensors and Actuators A: Physical 331: 113003. https://doi.org/10.1016/j.sna.2021.113003
- Lin, Y.-S., Yang, Z.-Y., Anand, A., Huang, C.-C. and Chang, H.-T., 2022. Carbon dots with polarity-tunable characteristics for the selective detection of sodium copper chlorophyllin and copper ions. Analytica Chimica Acta 1191: 339311. https://doi. org/10.1016/j.aca.2021.339311
- Liu, N. and Tang, M., 2020. Toxicity of different types of quantum dots to mammalian cells in vitro: an update review. Journal of Hazardous Materials 399: 122606. https://doi.org/10.1016/j. jhazmat.2020.122606
- Lu, L., Feng, C., Xu, J., Wang, F., Yu, H., Xu, Z. and Zhang, W., 2017. Hydrophobic-carbon-dot-based dual-emission micelle for ratiometric fluorescence biosensing and imaging of Cu²⁺ in liver cells. Biosensors and Bioelectronics 92: 101–108. https://doi.org/10.1016/j.bios.2017.01.066
- Mao, Q.-X., Shuang, E, Xia, J.-M., Song, R.-S., Shu, Y., Chen, X.-W. and Wang, J.-H., 2016. Hydrophobic carbon nanodots with

- rapid cell penetrability and tunable photoluminescence behavior for *in vitro* and *in vivo* imaging. Langmuir 32(46): 12221–12229. https://doi.org/10.1021/acs.langmuir.6b03331
- Mao, Q.-X., Wang, W.-J., Hai, X., Shu, Y., Chen, X.-W. and Wang, J.-H., 2015. The regulation of hydrophilicity and hydrophobicity of carbon dots via a one-pot approach. Journal of Materials Chemistry B 3: 6013–6018. https://doi.org/10.1039/ C5TB00963D
- Marković, Z.M., Kováčová, M., Humpolíček, P., Budimir, M.D., Vajďák, J., Kubát, P., Mičušík, M., Švajdlenková, H., Danko, M., Capáková, Z., Lehocký, M., Todorović Marković, B.M. and Špitalský, Z., 2019. Antibacterial photodynamic activity of carbon quantum dots/polydimethylsiloxane nanocomposites against Staphylococcus aureus, Escherichia coli and Klebsiella pneumoniae. Photodiagnosis and Photodynamic Therapy 26: 342–349. https://doi.org/10.1016/j.pdpdt.2019.04.019
- Marković, Z.M., Kováčová, M., Jeremić, S.R., Nagy, Š., Milivojević, D.D., Kubat, P., Kleinová, A., Budimir, M.D., Mojsin, M.M., Stevanović, M.J., Annušová, A., Špitalský, Z. and Todorović Marković, B.M., 2022. Highly efficient antibacterial polymer composites based on hydrophobic riboflavin carbon polymerized dots. Nanomaterials 12: 432. https://doi.org/10.3390/nano12224070
- Mauro, N., Utzeri, M.A., Drago, S.E., Nicosia, A., Costa, S., Cavallaro, G. and Giammona, G., 2021. Hyaluronic acid dressing of hydrophobic carbon nanodots: a self-assembling strategy of hybrid nanocomposites with theranostic potential. Carbohydrate Polymers 267: 118213. https://doi.org/10.1016/j. carbpol.2021.118213
- Mitra, S., Chandra, S., Kundu, T., Banerjee, R., Pramanik, P. and Goswami, A., 2012. Rapid microwave synthesis of fluorescent hydrophobic carbon dots. RSC Advances 2: 12129–12131. https://doi.org/10.1039/c2ra21048g
- Moldoveanu, S. and David, V., 2021. Phase transfer in sample preparation. In: Moldoveanu, S., David, V. (eds.). Modern sample preparation for chromatography. Elsevier, Amsterdam, the Netherlands, pp. 105–130. https://doi.org/10.1016/B978-0-12-821405-3.00011-3
- Mondal, T.K., Kapuria, A., Miah, M. and Saha, S.K., 2023. Solubility tuning of alkyl amine functionalized carbon quantum dots for selective detection of nitroexplosive. Carbon (N.Y.) 209: 117972. https://doi.org/10.1016/j.carbon.2023.03.047
- Moradi, M., Molaei, R., Kousheh, S.A., T. Guimarães, J. and McClements, D.J., 2023. Carbon dots synthesized from microorganisms and food by-products: active and smart food packaging applications. Critical Reviews in Food Science and Nutrition 63: 1943–1959. https://doi.org/10.1080/10408398.2021.2015283
- Mousavi Khaneghah, A., Hashemi, S.M.B. and Limbo, S., 2018. Antimicrobial agents and packaging systems in antimicrobial active food packaging: an overview of approaches and interactions. Food and Bioproducts Processing 111: 1–19. https://doi.org/10.1016/j.fbp.2018.05.001
- Ndlwana, L., Raleie, N., Dimpe, K.M., Ogutu, H.F., Oseghe, E.O., Motsa, M.M., Msagati, T.A.M. and Mamba, B.B., 2021. Sustainable hydrothermal and solvothermal synthesis of advanced carbon materials in multidimensional applications: a

- review. Materials (Basel). 14(17): 5094. https://doi.org/10.3390/ $\,$ ma14175094
- Pagidi, S., Sadhanala, H.K., Sharma, K. and Gedanken, A., 2022. One-pot synthesis of deep blue hydrophobic carbon dots with room temperature phosphorescence, white light emission, and explosive sensor. Advanced Electronic Materials 8: 2100969. https://doi.org/10.1002/aelm.202100969
- Paul, S., Bhattacharya, A., Hazra, N., Gayen, K., Sen, P. and Banerjee, A., 2022. Yellow-emitting carbon dots for selective fluorescence imaging of lipid droplets in living cells. Langmuir 38: 8829–8836. https://doi.org/10.1021/acs.langmuir.2c00919
- Prikhozhdenko, E.S., Bratashov, D.N., Mitrofanova, A.N., Sapelkin, A. V., Yashchenok, A.M., Sukhorukov, G.B. and Goryacheva, I.Y., 2018. Solvothermal synthesis of hydrophobic carbon dots in reversed micelles. Journal of Nanoparticle Research 20: 1–11. https://doi.org/10.1007/s11051-018-4336-x
- Puckowski, A., Mioduszewska, K., Łukaszewicz, P., Borecka, M., Caban, M., Maszkowska, J. and Stepnowski, P., 2016. Bioaccumulation and analytics of pharmaceutical residues in the environment: a review. Journal of Pharmaceutical and Biomedical Analysis 127: 232–255. https://doi.org/10.1016/j. jpba.2016.02.049
- Qu, S., Zhou, D., Li, D., Ji, W., Jing, P., Han, D., Liu, L., Zeng, H. and Shen, D., 2016. Toward efficient orange emissive carbon nanodots through conjugated sp2-domain controlling and surface charges engineering. Advanced Materials 28: 3516–3521. https://doi.org/10.1002/adma.201504891
- Raveendran, V. and Kizhakayil, R.N., 2021. Fluorescent carbon dots as biosensor, green reductant, and biomarker. ACS Omega 6: 23475–23484. https://doi.org/10.1021/acsomega.1c03481
- Razavi, R., Tajik, H., Molaei, R., McClements, D.J. and Moradi, M., 2024. Janus nanoparticles synthesized from hydrophobic carbon dots and carboxymethyl cellulose: novel antimicrobial additives for fresh food applications. Food Bioscience 62: 105171. https:// doi.org/10.1016/j.fbio.2024.105171
- Shang, W., Ye, M., Cai, T., Zhao, L., Zhang, Y., Liu, D. and Liu, S., 2018. Tuning of the hydrophilicity and hydrophobicity of nitrogen doped carbon dots: a facile approach towards high efficient lubricant nanoadditives. Journal of Molecular Liquids 266: 65–74. https://doi.org/10.1016/j.molliq.2018.06.042
- Shebeeb, C.M., Joseph, A., Farzeena, C., Dinesh, R. and Sajith, V., 2022. Fluorescent carbon dot embedded polystyrene particle: an alternative to fluorescently tagged polystyrene for fate of microplastic studies: a preliminary investigation. Applied Nanoscience 12: 2725–2731. https://doi.org/10.1007/s13204-022-02566-8
- Shi, X., Wang, X., Zhang, S., Zhang, Z., Meng, X., Liu, H., Qian, Y., Lin, Y., Yu, Y., Lin, W. and Wang, H., 2023. Hydrophobic carbon dots derived from organic pollutants and applications in NIR anticounterfeiting and bioimaging. Langmuir 39: 5056–5064. https://doi.org/10.1021/acs.langmuir.3c00075
- Shi, X., Wei, W., Fu, Z., Gao, W., Zhang, C., Zhao, Q., Deng, F. and Lu, X., 2019. Review on carbon dots in food safety applications. Talanta 194: 809–821. https://doi.org/10.1016/j.talanta.2018.11.005
- Shinde, V.R., Khatun, S., Thanekar, A.M., Hak, A. and Rengan, A.K., 2023. Lipid-coated red fluorescent carbon dots for imaging and

- synergistic phototherapy in breast cancer. Photodiagnosis and Photodynamic Therapy 41: 103314. https://doi.org/10.1016/j.pdpdt.2023.103314
- Shu, Y., Lu, J., Mao, Q.-X., Song, R.-S., Wang, X.-Y., Chen, X.-W. and Wang, J.-H., 2017. Ionic liquid-mediated organophilic carbon dots for drug delivery and bioimaging. Carbon (N.Y.). 114: 324–333. https://doi.org/10.1016/j.carbon.2016.12.038
- Stanković, N.K., Bodik, M., Šiffalovič, P., Kotlar, M. and Mičušik, M., 2018. Antibacterial and antibiofouling properties of light triggered fluorescent hydrophobic carbon quantum dots Langmuir–Blodgett thin films. ACS Sustainable Chemistry & Engineering 6(3): 4154–4163. https://doi. org/10.1021/acssuschemeng.7b04566
- Sun, Y., Zhang, M., Bhandari, B. and Yang, C., 2022. Recent development of carbon quantum dots: biological toxicity, antibacterial properties and application in foods. Food Reviews International 38: 1513–1532. https://doi.org/10.1080/87559129.2020.1818255
- Tajik, S., Dourandish, Z., Zhang, K., Beitollahi, H., Quyet, B., Le, V., Ho, E., Jang, W. and Shokouhimehr, M., 2020. Carbon and graphene quantum dots: a review on syntheses, characterization, biological and sensing applications for neurotransmitter determination. RSC Advances 10(26):15406–15429. https://doi. org/10.1039/d0ra00799d
- Talib, A., Pandey, S., Thakur, M. and Wu, H.-F., 2015. Synthesis of highly fluorescent hydrophobic carbon dots by hot injection method using Paraplast as precursor. Materials Science and Engineering: C 48: 700–703. https://doi.org/10.1016/j.msec.2014.11.058
- Taylor, N., Ma, W., Kristopeit, A., Wang, S. and Zydney, A.L., 2022. Evaluating nanoparticle hydrophobicity using analytical membrane hydrophobic interaction chromatography. Analytical Chemistry 94: 8668–8673. https://doi.org/10.1021/acs.analchem.2c00710
- Varisco, M., Zufferey, D., Ruggi, A., Zhang, Y., Erni, R. and Mamula, O., 2017. Synthesis of hydrophilic and hydrophobic carbon quantum dots from waste of wine fermentation. Royal Society Open Science 4: 170900. https://doi.org/10.1098/rsos.170900
- Wang, Z., Liu, Y., Liang, M., Chen, Y., Dong, W., Hu, Q., Song, S., Shuang, S., Dong, C. and Gong, X., 2024. Hydrophobic carbon quantum dots with red fluorescence: an optical dualmode and smartphone imaging sensor for identifying Chinese Baijiu quality. Talanta 275: 126064. https://doi.org/10.1016/j. talanta.2024.126064
- Wang, J.-L., Teng, J.-Y., Jia, T. and Shu, Y., 2018. Detection of yeast Saccharomyces cerevisiae with ionic liquid mediated carbon dots. Talanta 178: 818–824. https://doi.org/10.1016/j. talanta.2017.10.029
- Wen, Y., Jia, Q., Nan, F., Zheng, X., Liu, W., Wu, J., Ren, H., Ge, J. and Wang, P., 2019. Pheophytin derived near-infrared-light responsive carbon dot assembly as a new phototheranotic agent for bioimaging and photodynamic therapy. Chemistry: An Asian Journal 14: 2162–2168. https://doi.org/10.1002/asia.201900416
- Wu, M., Zhan, J., Geng, B., He, P., Wu, K., Wang, L., Xu, G., Li, Z., Yin, L. and Pan, D., 2017. Scalable synthesis of organic-soluble carbon quantum dots: superior optical properties in solvents, solids, and LEDs. Nanoscale 9: 13195–13202. https://doi.org/10.1039/C7NR04718E

- Xu, J., Zhang, Y., Guo, X., Zhang, H., Deng, Y. and Zhao, X., 2023.
 Aggregation-induced emission solid-state multicolor fluorescent carbon dots for LEDs and fingerprints applications.
 Journal of Luminescence 256: 119625. https://doi.org/10.1016/j.jlumin.2022.119625
- Yang, J.-C., Gao, S., Zhang, J.-H., Lv, H.-T. and Wu, Q., 2022. Ionic liquid and octadecylamine co-derived carbon dots for multi-mode high performance liquid chromatography. Microchemical Journal 182: 107932. https://doi.org/10.1016/j. microc.2022.107932
- Yang, H., Liu, Y., Guo, Z., Lei, B., Zhuang, J., Zhang, X., Liu, Z. and Hu, C., 2019. Hydrophobic carbon dots with blue dispersed emission and red aggregation-induced emission. Nature Communications 10: 1789. https://doi.org/10.1038/s41467-019-09830-6
- Yang, J., Zhang, X., Ma, Y.-H., Gao, G., Chen, X., Jia, H.-R., Li, Y.-H., Chen, Z. and Wu, F.-G., 2016. Carbon dot-based platform for simultaneous bacterial distinguishment and antibacterial applications. ACS Applied Materials & Interfaces 8: 32170–32181. https://doi.org/10.1021/acsami.6b10398
- Yao, B., Huang, H., Liu, Y. and Kang, Z., 2019. Carbon dots: a small conundrum. Trends in Chemistry 1: 235–246. https://doi. org/10.1016/j.trechm.2019.02.003
- Yen, Y.-T., Lin, Y.-S., Chen, T.-H., Chyueh, S.-C. and Chang, H.-T., 2020. A carbon-dot sensing probe for screening of date rape drugs: nitro-containing benzodiazepines. Sensors and Actuators, B: Chemical 305: 127441. https://doi.org/10.1016/j. snb.2019.127441
- Yin, K., Lu, D., Wang, L., Zhang, Q., Hao, J., Li, G. and Li, H., 2019. Hydrophobic carbon dots from aliphatic compounds with one terminal functional group. Journal of Physical Chemistry C 123: 22447–22456. https://doi.org/10.1021/acs.jpcc.9b04479
- Zhan, J., Geng, B., Wu, K., Xu, G., Wang, L., Guo, R., Lei, B., Zheng, F., Pan, D. and Wu, M., 2018. A solvent-engineered molecule fusion strategy for rational synthesis of carbon quantum dots with multicolor bandgap fluorescence. Carbon (N.Y.) 130: 153–163. https://doi.org/10.1016/j.carbon.2017.12.075
- Zhang, Z., Hu, J., Liu, S., Hao, X., Li, L., Zou, G., Hou, H. and Ji, X., 2021. Channel regulation of TFC membrane with hydrophobic carbon dots in forward osmosis. Chinese Chemical Letters 32: 2882–2886. https://doi.org/10.1016/j.cclet.2021.03.028
- Zhang, S., Li, B., Zhou, J., Shi, J., He, Z., Zhao, Y., Li, Y., Shen, Y., Zhang, Y. and Wu, S., 2023a. Kill three birds with one stone:

- mitochondria-localized tea saponin derived carbon dots with AIE properties for stable detection of HSA and extremely acidic pH. Food Chemistry 405: 134865. https://doi.org/10.1016/j.foodchem.2022.134865
- Zhang, J., Liu, X., Wang, X., Mu, L., Yuan, M., Liu, B. and Shi, H., 2018. Carbon dots-decorated Na2W4O13 composite with WO3 for highly efficient photocatalytic antibacterial activity. Journal of Hazardous Materials 359: 1–8. https://doi.org/10.1016/j. jhazmat.2018.06.072
- Zhang, W., Sigdel, G., Mintz, K.J., Seven, E.S., Zhou, Y., Wang, C. and Leblanc, R.M., 2021. Carbon dots: a future blood-brain barrier penetrating nanomedicine and drug nanocarrier. International Journal of Nanomedicine 16: 5003–5016. https://doi.org/10.2147/IJN.S318732
- Zhang, W., Sun, D.-W., Ma, J., Qin, A. and Tang, B.Z., 2023b. A ratiometric fluorescent tag based on dual-emissive hydrophobic carbon dots for *in situ* monitoring of seafood freshness. Analytica Chimica Acta 1250: 340931. https://doi.org/10.1016/j.aca.2023.340931
- Zhang, C., Ying, Z., Jiang, Y., Wang, H., Zhou, X., Xuan, W. and Zheng, P., 2024. Solvent-controlled synthesis of hydrophilic and hydrophobic carbon dots. Physical Chemistry Chemical Physics 26: 314–322. https://doi.org/10.1039/D3CP04273A
- Zhao, D., Zhang, Z., Li, C., Xiao, X., Li, J., Liu, X. and Cheng, H., 2020. Yellow-emitting hydrophobic carbon dots via solid-phase synthesis and their applications. ACS Omega 5: 22587–22595. https://doi.org/10.1021/acsomega.0c03239
- Zheng, B., Liu, X., Hu, J., Wang, F., Hu, X., Zhu, Y., Lv, X., Du, J. and Xiao, D., 2019. Construction of hydrophobic interface on natural biomaterials for higher efficient and reversible radioactive iodine adsorption in water. Journal of Hazardous Materials 368: 81–89. https://doi.org/10.1016/j.jhazmat.2019.01.037
- Zheng, B., Liu, T., Paau, M.C., Wang, M., Liu, Y., Liu, L., Wu, C., Du, J., Xiao, D. and Choi M.M.F., 2015. One pot selective synthesis of water and organic soluble carbon dots with green fluorescence emission. RSC Advances 5: 11667–11675. https://doi.org/10.1039/C4RA16529B
- Zhou, Y., Liyanage, P.Y., Devadoss, D., Guevara, L.R.R., Cheng, L., Graham, R.M., Chand, H.S., Al-Youbi, A.O., Bashammakh, A.S. and El-Shahawi, M.S., 2019. Nontoxic amphiphilic carbon dots as promising drug nanocarriers across the blood–brain barrier and inhibitors of β -amyloid. Nanoscale 11: 22387–22397. https://doi.org/10.1039/c9nr08194a